ARTICLE

Confidence Intervals for the Reliability of Dependent Systems: Integrating Frailty Models and Copula-Based Methods

Osnamir E. Bru-Cordero[1] **, Cecilia Castro**[2] **, Víctor Leiva**[3,*] **and Mario C. Jaramillo-Elorza**[4]

[1]Dirección Académica, Universidad Nacional de Colombia, Sede De La Paz, La Paz, Cesar, 202010, Colombia
[2]Centre of Mathematics, Universidade do Minho, Braga, 4710-057, Portugal
[3]Escuela de Ingeniería Industrial, Pontificia Universidad Católica de Valparaíso, Valparaíso, 2362807, Chile
[4]Departamento de Estadística, Universidad Nacional de Colombia, Sede Medellín, Medellín, 050023, Colombia
*Corresponding Author: Víctor Leiva. Emails: victor.leiva@pucv.cl or victorleivasanchez@gmail.com

ABSTRACT: Most reliability studies assume large samples or independence among components, but these assumptions often fail in practice, leading to imprecise inference. We address this issue by constructing confidence intervals (CIs) for the reliability of two-component systems with Weibull distributed failure times under a copula-frailty framework. Our construction integrates gamma-distributed frailties to capture unobserved heterogeneity and a copula-based dependence structure for correlated failures. The main contribution of this work is to derive adjusted CIs that explicitly incorporate the copula parameter in the variance-covariance matrix, achieving near-nominal coverage probabilities even in small samples or highly dependent settings. Through simulation studies, we show that, although traditional methods may suffice with moderate dependence and large samples, the proposed CIs offer notable benefits when dependence is strong or data are sparse. We further illustrate our construction with a synthetic example illustrating how penalized estimation can mitigate the issue of a degenerate Hessian matrix under high dependence and limited observations, so enabling uncertainty quantification despite deviations from nominal assumptions. Overall, our results fill a gap in reliability modeling for systems prone to correlated failures, and contribute to more robust inference in engineering, industrial, and biomedical applications.

KEYWORDS: Censored data; copula methods; dependent failure times; interval estimation; Weibull distribution

1 Introduction

Reliability is essential for the continuous operation of modern engineering and technological systems, particularly in sectors where uninterrupted service is vital to safety and efficiency [1–3]. Critical infrastructures, such as power grids, transportation networks, and healthcare systems, depend on uninterrupted functionality to mitigate severe consequences such as power outages, transportation disruptions, and failures of medical devices, which can lead to loss of life, economic damage, or environmental harm. Recent advances in areas such as blockchain technology [4] and robust statistical methods for geostatistical data [5] have contributed to improving the reliability of these essential systems. A key challenge in reliability analysis is to capture the interdependence of system components, often referred to as common mode failures [6].

Although the assumption of independence is commonly made for mathematical convenience, it can produce an issue of imprecise inference when components share factors or conditions that increase the probability of simultaneous or correlated failures. To address this issue, researchers have proposed various models that move beyond strict independence. For instance, composable modeling techniques have been used to describe complex systems [7], and methods like Monte Carlo simulation [8] help to manage structural dependence [9].

Advances on the topic have been proposed. Functional links between components—represented, for example, in failure-tree or block-diagram models—underscore the complexity of accurate reliability estimation with dependence [7,10]. Although redundancy is used to improve reliability, it may exacerbate underestimation when components share covariates [11–14]. Copula methods are suited to modeling correlated structures in competing risks [1,15] and positive dependence among components, which is critical for realistic analysis [16–20].

Despite these advances, there remains a gap in constructing accurate confidence intervals (CIs) for small-scale series systems with strong dependence, as many existing studies focus on larger systems or making simplifying assumptions [21]. In a two-component series system, the overall failure occurs at whichever component fails first. When the two components are positively correlated, one typically observes low reliability because an early failure in one component is more likely to coincide with an early failure in the other, resulting in a shorter overall system failure time. Although copula-based methods and frailty models have been extensively examined [22–26], recent work proposes further generalizations to multivariate or cured-fraction settings [27,28], highlighting the broader potential of combining copula-based methods and frailty models. However, their integration in small-sample series systems remains relatively unexplored.

Building on the likelihood-based frailty-copula framework for competing risks proposed in [24], we extend that framework by incorporating a gamma distributed frailty term [29] into a two-component system, where the failure time of each component follows a Weibull distribution [30,31]. Our key innovation lies in capturing both unobserved heterogeneity and conditional association via a Gumbel copula. By examining varying dependence levels and sample sizes, we show how these two sources of correlation—frailty variance and copula-based tail dependence—affect the accuracy of inference under challenging yet practically relevant conditions. Also, we present a penalized-estimation case study designed to mimic a real-world scenario where unexpectedly high dependence or sparse data can cause the Hessian matrix to degenerate under the maximum likelihood (ML) method. This case study is an illustrative example that underscores how our framework can still yield interval estimates (albeit with potential bias) when real data are not available and small-sample issues are severe.

Throughout the article, we use a consistent set of symbols and acronyms, which are listed in Table 1 in the order of first appearance. Sections are arranged as follows. Section 2 provides background of copula-based methods and frailty models for reliability analysis. In Section 3, we describe the methodology for modeling competing risks data. In Section 4, CIs are constructed for dependent systems under ML estimation and delta-method. Section 5 conducts simulations, showing the roles of dependence and censoring in coverage probabilities (CPs) for Weibull-distributed failure times. In Section 6, we offer a synthetic example illustrating how penalized estimation can handle degenerate Hessian matrices under strong dependence and small samples. Section 7 concludes with findings and ideas for future research.

2 Theoretical Background

In this section, we present two main approaches in reliability analysis: copula-based methods for capturing dependence and frailty models for handling unobserved heterogeneity. These approaches form the basis for our proposed competing risks model with dependent failure times.

Table 1: Notation used throughout the article (in order of first appearance) in all the cases with $i \in \{1, \ldots, n\}$ and $j \in \{1, 2\}$

Symbol	Definition/Description
rule n	Total number of independent units (or items/components) under study.
T_{ij}	Failure time of mode j for unit i.
δ_{ij}	Indicator with $\delta_{ij} = 1$ if unit i fails due to mode j, and $\delta_{ij} = 0$ otherwise.
t_i	Observed failure time for unit i.
Z_i	Frailty for unit i, assumed $Z_i \sim \text{Gamma}\,(1/\eta, \eta)$ independent and identically distributed.
η	Variance parameter of the frailty distribution, denoted as $\text{Var}[Z_i] = \eta$.
α_j	Shape parameter of the Weibull distribution for the failure time of mode j.
λ_j	Scale parameter of the Weibull distribution for the failure time of mode j.
α, λ	Generic notation for shape α and scale λ parameters of Weibull distributions, when the subscript j is implicit.
CDF	Cumulative distribution function
$F_{T_{ij}}(t), S_{T_{ij}}(t)$	Marginal CDF and survival function for failure time T_{ij}.
$C_\theta(T_{i1}, T_{i2})$	Bivariate copula function with parameter θ for modeling dependence between T_{i1} and T_{i2}.
θ	Gumbel copula parameter, where $\theta \geq 1$.
τ	Nonparametric measure of association named the Kendall tau.
$S_{T_{i1}, T_{i2}}(t_1, t_2)$	Joint survival function of between T_{i1} and T_{i2}, that is, $\Pr(T_{i1} > t_1, T_{i2} > t_2)$.
$f(t_i, j)$	Density contribution at time t_i for mode j in the likelihood function if $\delta_{ij} = 1$.
$L(\boldsymbol{\theta}), \ell(\boldsymbol{\theta})$	Likelihood and log-likelihood functions, where $\boldsymbol{\theta} = (\alpha_1, \lambda_1, \alpha_2, \lambda_2, \eta, \theta)$.
$\widehat{\boldsymbol{\theta}}$	Maximum likelihood (ML) estimator of the parameter vector $\boldsymbol{\theta}$.
$\widehat{\Sigma}$	Estimated covariance matrix via the Fisher information for $\widehat{\boldsymbol{\theta}}$.
$t_{p,j}$	p-th percentile (quantile) of the marginal distribution of T_{ij}, with $0 < p < 1$.
p	Probability level for quantiles or survival in reliability, such as $p \in \{0.05, 0.50, 0.95\}$.
$\widehat{t}_{p,j}, \widehat{y}_{p,j} = \log(\widehat{t}_{p,j})$	Estimated quantile and its log-transform, used for constructing CIs for the reliability of failure mode j.
$\text{CI}(t_{p,j})$	Confidence interval (CI) for the p-th percentile $t_{p,j}$.
α_{CI}	Significance level used in constructing $(1 - \alpha_{\text{CI}}) \times 100\%$ CIs.
n_j, r_j	Sample size (n_j) and number of observed failures (r_j) for mode j.
SE	Standard error.
MTTF	Mean time to failure which summarizes reliability at the system level.

2.1 Copula-Based Methods for Dependency Structures

Copula-based methods are especially helpful for modeling the system reliability when component failures are dependent. These methods allow analysts to separate the marginal failure-time behavior from the joint dependence structure. Such methods are essential in real-world applications, where the assumption of independence among components is often unrealistic.

In essence, a copula is a bivariate cumulative distribution function (CDF) defined on the unit square $\mathcal{I}^2 \equiv [0, 1]^2$, which connects marginal distributions to form a joint distribution [18]. This is helpful

in reliability problems where component failure times are correlated in ways that independent models cannot capture.

Definition 1: *A bivariate copula is a function $C: \mathcal{I}^2 \to \mathcal{I} \equiv [0,1]$, satisfying:*

(*i*)   *Boundary conditions–For all $u \in \mathcal{I}$, $C(0, u) = C(u, 0) = 0$ and $C(1, u) = C(u, 1) = u$.*

(*ii*) *Two-increasing property–For all $0 \le u_1 < u_2 \le 1$ and $0 \le v_1 < v_2 \le 1$, $C(u_2, v_2) - C(u_1, v_2) - C(u_2, v_1) + C(u_1, v_1) \ge 0$.*

Definition 1 ensures that the copula encodes the dependence between two random variables.

Because a copula has uniform marginals on $[0, 1]$, it effectively couples the one-dimensional distributions to form the joint distribution -a concept widely applied in reliability, finance, and other fields [32]. A fundamental result in copula theory is the Sklar theorem given next.

Theorem 1 (Sklar)**:** *Let T_1 and T_2 be random variables with joint CDF F and marginal CDFs F_1 and F_2, respectively. Then, there exists a copula C such that $F(t_1, t_2) = C(F_1(t_1), F_2(t_2))$. If F_1 and F_2 are continuous, C is unique. Conversely, for any copula C and continuous marginal CDFs F_1, F_2, the function $(t_1, t_2) \mapsto C(F_1(t_1), F_2(t_2))$ is a valid joint CDF.*

The Sklar result presented in Theorem 1 underpins much of copula theory by separating marginal distributions from the dependence structure. This remains true in bivariate and multivariate contexts [18].

Corollary 1: *Let F be a joint CDF of (T_1, T_2) with continuous marginal CDFs F_1 and F_2. Then, the associated copula can be expressed as $C(u, v) = F(F_1^{-1}(u), F_2^{-1}(v))$, where F_j^{-1} denotes the quantile (or pseudo-inverse) function of F_j. Consequently, if F_1 and F_2 are the marginal CDFs, C serves as the joint CDF of $(U, V) = (F_1(T_1), F_2(T_2))$, which are uniformly distributed on $[0, 1]$.*

An immediate implication of the Sklar theorem is that the product copula $\Pi(u, v) = uv$ fully characterizes the joint distribution of two independent random variables. Any deviation from this product implies dependence between the variables. In practice, more flexible copulas—such as Clayton, Frank, or Gumbel—are often needed to capture complex dependence patterns.

2.2 Frailty Models for Failure Times in Competing Risks

Traditional reliability analysis often assumes that failure times are mutually independent. However, this assumption is frequently violated in systems where dependence exists. Correlated frailty models, as discussed in [33], offer a convenient framework for incorporating such dependence.

Parametric and semiparametric Bayesian frailty models [34] also handle shared risks effectively. Moreover, various estimation and extension approaches (such as the expectation-maximization algorithm for semiparametric hazards [35], and the developments presented in [36,37]) further enhance the modeling of correlated failure times under frailty frameworks.

A typical frailty model consists of three main parts as follows [38]:

- A frailty term representing latent or unobserved heterogeneity.
- A baseline risk function, which can be either parametric or nonparametric.
- An optional fixed-effects term to incorporate observed covariates.

Based on [24], we adopt a gamma distributed frailty to account for unobserved heterogeneity when modeling the failure times of two components using the Weibull distribution under competing risks. This adoption captures additional dependence arising from latent factors that affect both modes of failure in a single unit. In addition, we adapt the CI construction proposed in [39] to incorporate both the covariance structure of our frailty model and the dependence parameter of the copula. This provides a robust framework for inference on the system reliability when failure times are dependent.

In many real scenarios involving multiple competing risks, accurately capturing the interplay between shared risks (through a frailty) and direct dependence (through a copula) is critical. Therefore, we propose a framework merging both frailty and copula components to achieve a comprehensive characterization of the system reliability with dependent competing failure modes.

2.3 Advantages of the Proposed Framework

By combining a gamma-distributed frailty with a specific copula (here, the Gumbel family), our frailty-copula approach offers the following advantages:

- It captures unobserved heterogeneity through the latent variable Z_i, for $i \in \{1, \ldots, n\}$, allowing certain units to be more frail or more robust without explicit covariates.
- It enables conditional tail dependence beyond what a simple frailty model can account for—an effect introduced through the Gumbel copula structure. This is especially valuable in high-risk scenarios where correlated early failures can occur more often than basic models suggest.

These two sources of dependence –the gamma distributed frailty Z_i and the Gumbel copula parameter θ– provide complementary ways to model correlation. Specifically, θ measures the conditional association (such as the Kendall tau, $\tau = 1 - 1/\theta$) given $Z_i = z$, for $i \in \{1, \ldots, n\}$, whereas the variance η of Z_i also influences the marginal (overall) correlation observed in the data. Hence, if $\eta > 0$, the total correlation can differ from $1 - 1/\theta$ when viewed unconditionally. Such a dual-layered perspective is particularly relevant when real-world factors create both large heterogeneity across units and direct dependence among components or failure modes.

3 Modeling Competing Risks with Dependent Failure Times

In this section, we first present and adapt the frailty-copula framework introduced in [24], focusing on a two-component system with Weibull distributed failure times under competing risks. Then, we go beyond [24] by deriving CIs for marginal quantiles via a log-transformed delta method, fully incorporating both the frailty parameter η and the copula parameter θ.

3.1 Competing Risks Model with Gamma Distributed Frailty and Gumbel Copula

In reliability terms, two failure time variables, T_{i1} and T_{i2} say, for $i \in \{1, \ldots, n\}$, may be interpreted in two ways: (i) as two possible modes of failure (competing risks) acting on the same item; or (ii) as two physical components arranged in series, that is, the system fails at $\min_i\{T_{i1}, T_{i2}\}$. Mathematically, both ways involve observing whichever occurs first, but the practical interpretation (one item with multiple risks versus a two-component system) depends on the engineering or biomedical context.

We adopt the Weibull distribution for each failure time, due to its well-established versatility in reliability contexts. It is capable of modeling various hazard shapes, such as increasing, constant, or decreasing failure rates. Nevertheless, our frailty-copula construction is not intrinsically limited to the Weibull model. In principle, other parametric forms—such as a generalized linear exponential distribution—could be used if prior knowledge or data analyses suggest a hazard structure not adequately captured by the Weibull model. In practice, implementing such alternatives often requires re-deriving the likelihood contributions for the copula-frailty model, which may lead to integrals without closed-form solutions and additional numerical complexity.

Moreover, with small sample sizes or strong dependence, identifiability of the extra parameters can pose further challenges. Given the broad applicability and familiarity of the Weibull model in engineering, we focus on that baseline here, noting that extensions to other parametric families remain viable future avenues

under the same modeling framework. Hence, within this formulation based on the Weibull distribution, each failure time T_{i1} or T_{i2}, for $i \in \{1, \ldots, n\}$, is still governed by the same gamma distributed frailty and copula structure described below. In practice, only the earliest failure time is observed (along with its corresponding failure mode), while the remaining mode is censored at that same time.

The proposed model accounts for two distinct sources of dependence: (i) unobserved heterogeneity, captured by a gamma distributed frailty Z_i, for $i \in \{1, \ldots, n\}$. This allows, as mentioned, certain units to be more frail or more robust, reflecting latent factors not explained by observable covariates; (ii) conditional tail dependence, introduced via a Gumbel copula. Even after controlling for the shared frailty, correlated failure times can occur more frequently than predicted by a simple gamma distributed mixture alone. This is particularly relevant in high-risk scenarios where early failures tend to cluster.

In this study, we mainly adopt the viewpoint of two failure modes competing for the same item, but our formulas also apply to a two-component series arrangement with minimal modifications.

The Weibull distributed baseline and other options are considered next. Following [24] and usual practice in reliability studies, we adopt a Weibull distribution for each failure time. This adoption is motivated by the flexibility of the Weibull model in describing a range of hazard shapes and its common usage in engineering contexts. Although we focus on the Weibull distribution here, the framework can accommodate other parametric baselines (for example, exponential, gamma, generalized linear hazard distributions), or even semiparametric models, if domain knowledge or data characteristics suggest a different modeling strategy. In particular, a generalized linear exponential distribution could also be utilized within the same frailty-copula structure, albeit with different hazard formulations and potentially more challenging estimation details.

Next, we describe the gamma-distributed frailty. We introduce a gamma distributed frailty variable Z_i, independently drawn for unit i, with $i \in \{1, \ldots, n\}$, to account for unobserved shared risk factors. Specifically, we assume that $Z_i \sim \text{Gamma}(1/\eta, \eta)$, with $\mathbb{E}[Z_i] = 1$ and $\text{Var}[Z_i] = \eta$. Thus, the frailty term Z_i represents the unit-specific unobserved heterogeneity, where values greater than one indicate higher susceptibility (greater frailty), and values below one are units with lower risk (more robust).

Given $Z_i = z$, each failure time T_{ij}, for mode $j \in \{1, 2\}$, follows a Weibull distribution with shape $\alpha_j > 0$ and scale $\lambda_j > 0$. Thus, the conditional survival function of T_{ij} is given by

$$S_{T_{ij}Z_i = z}(t) = \exp\left(-z\left(\frac{t}{\lambda_j}\right)^{\alpha_j}\right), \quad t > 0.$$

To induce dependence between T_{i1} and T_{i2} conditional on $Z_i = z$, we employ the Gumbel copula stated as

$$C_\theta(u, v) = \exp\left(-\left((-\log(u))^\theta + (-\log(v))^\theta\right)^{1/\theta}\right), \quad (u, v) \in (0, 1)^2, \theta \geq 1.$$

Hence, the joint conditional survival function of (T_{i1}, T_{i2}) given $Z_i = z$ is formulated as $S_{T_{i1}, T_{i2} Z_i = z}(t_1, t_2) = C_\theta\left(S_{T_{i1}Z_i = z}(t_1), S_{T_{i2}Z_i = z}(t_2)\right)$, for $t_1 > 0, t_2 > 0$. To obtain the unconditional joint survival function for (T_{i1}, T_{i2}), we integrate out the frailty Z_i via the expression defined as $S_{T_{i1}, T_{i2}}(t_1, t_2) = \int_0^\infty S_{T_{i1}, T_{i2}Z_i = z}(t_1, t_2) f_{Z_i}(z) \mathrm{d}z$, for $t_1 > 0, t_2 > 0$, where f_{Z_i} is the gamma density with shape $1/\eta$ and scale η. Because the above integral generally lacks a closed-form expression, numerical or simulation-based techniques are required for practical inference [40,41].

Remark [Model identifiability]: Including both the gamma-frailty variance η and the Gumbel copula parameter θ in the model can raise identifiability issues when sample sizes are small or when covariate

information is limited [33,38]. In such scenarios, additional structure (such as repeated observations per unit or covariates) may be needed to separate unobserved heterogeneity from direct dependence.

Some implications and special cases are the following. Our frailty-copula method captures two complementary types of dependence: (i) extra-multiplier risk factors via Z_i (unobserved heterogeneity), and (ii) conditional tail dependence via the copula. A simpler special case arises if we assume conditional independence given $Z_i = z$, that is, $S_{T_{i1}, T_{i2} Z_i = z}(t_1, t_2) = S_{T_{i1} Z_i = z}(t_1) S_{T_{i2} Z_i = z}(t_2)$. Under Weibull distributed marginals plus gamma distributed frailty, this leads to a known closed-form for the unconditional joint survival [38] stated as

$$S_{T_{i1}, T_{i2}}(t_1, t_2) = \left(1 + \eta \left(\frac{t_1}{\lambda_1}\right)^{\alpha_1} + \eta \left(\frac{t_2}{\lambda_2}\right)^{\alpha_2}\right)^{-1/\eta}.$$

Even though this independence assumption given $Z_i = z$ eliminates direct copula-based dependence, the shared frailty η can still induce marginal correlation among (T_{i1}, T_{i2}).

3.2 Marginal Survival and Quantiles

Regardless of the specific copula, the marginal survival function for mode j follows from integrating out the frailty as

$$S_{T_j}(t) = \int_0^\infty \exp\left(-z \left(\frac{t}{\lambda_j}\right)^{\alpha_j}\right) f_Z(z) \mathrm{d}z = \left(1 + \eta \left(\frac{t}{\lambda_j}\right)^{\alpha_j}\right)^{-1/\eta}, \quad t > 0.$$

Hence, the marginal p-th quantile $t_{p,j}$ satisfies $S_{T_j}(t_{p,j}) = 1 - p$, which implies

$$t_{p,j} = \lambda_j \left(\frac{(1-p)^{-\eta} - 1}{\eta}\right)^{\frac{1}{\alpha_j}}, \quad 0 < p < 1. \tag{1}$$

Thus, although the joint distribution may be complex, the marginal survival functions and quantiles emerge in closed form. This feature proves convenient for constructing reliability-based CIs and for evaluating system-level performance measures.

3.3 Mean and Variance of Marginal Failure Times

In the simpler gamma-Weibull mixture model setting, where each unit experiences a single failure mode and no additional copula structure is introduced, closed-form expressions for the mean and variance of the marginal failure times can be obtained.

Consider the shape and scale parameters $\alpha_j > 0$ and $\lambda_j > 0$ of the Weibull distribution conditional on the gamma distributed frailty Z_i, and let $\eta > 0$ be the variance of the gamma distributed frailty, $Z_i \sim \text{Gamma}(1/\eta, \eta)$. It is established [33,38] that for integer values m satisfying $m/\alpha_j < 1/\eta$, a general expression for the m-th moment, and from this the first and second moments, are given, for $i \in \{1, \ldots, n\}$ and $j \in \{1, 2\}$, by

$$\mathbb{E}[T_{ij}^m] = \frac{\lambda_j^m \Gamma\left(\frac{1}{\eta} - \frac{m}{\alpha_j}\right) \Gamma\left(1 + \frac{m}{\alpha_j}\right)}{\Gamma\left(\frac{1}{\eta} + 1\right)}, \mathbb{E}[T_{ij}] = \frac{\lambda_j \Gamma\left(\frac{1}{\eta} - \frac{1}{\alpha_j}\right) \Gamma\left(1 + \frac{1}{\alpha_j}\right)}{\Gamma\left(\frac{1}{\eta} + 1\right)}, \mathbb{E}[T_{ij}^2] = \frac{\lambda_j^2 \Gamma\left(\frac{1}{\eta} - \frac{2}{\alpha_j}\right) \Gamma\left(1 + \frac{2}{\alpha_j}\right)}{\Gamma\left(\frac{1}{\eta} + 1\right)}.$$

Then, the variance follows immediately, for $i \in \{1, \ldots, n\}$ and $j \in \{1, 2\}$, as

$$\mathrm{Var}[T_{ij}] = \mathbb{E}[T_{ij}^2] - \left(\mathbb{E}[T_{ij}]\right)^2 = \frac{\lambda_j^2 \Gamma\left(\frac{1}{\eta} - \frac{2}{\alpha_j}\right)\Gamma\left(1 + \frac{2}{\alpha_j}\right)}{\Gamma\left(\frac{1}{\eta} + 1\right)} - \left(\frac{\lambda_j \Gamma\left(\frac{1}{\eta} - \frac{1}{\alpha_j}\right)\Gamma\left(1 + \frac{1}{\alpha_j}\right)}{\Gamma\left(\frac{1}{\eta} + 1\right)}\right)^2.$$

Note that, as η increases, both $\mathbb{E}[T_{ij}]$ and $\mathrm{Var}[T_{ij}]$ increase, for $i \in \{1, \ldots, n\}$ and $j \in \{1, 2\}$, reflecting greater unobserved heterogeneity among the units. High values of η also result in increased marginal correlation among the failure times T_{i1} and T_{i2}, even without an explicit copula parameter such as θ.

3.4 Dependence Structure and Identifiability in Competing Risks

Introducing a Gumbel copula C_θ conditional on the gamma distributed frailty Z_i does not alter the marginal distributions of each failure time associated with mode j. Indeed, the univariate survival functions remain stated as

$$S_{T_{ij}}(t) = \int_0^\infty \exp\left(-z\left(\frac{t}{\lambda_j}\right)^{\alpha_j}\right) f_Z(z)\mathrm{d}z, \quad t > 0, i \in \{1, \ldots, n\}, j \in \{1, 2\}.$$

where f_Z, as mentioned, is the gamma distributed frailty density. However, once the copula is introduced, the joint survival function is presented as

$$S_{T_{i1}, T_{i2}}(t_1, t_2) = \int_0^\infty C_\theta\left(\exp\left(-z\left(\frac{t_1}{\lambda_1}\right)^{\alpha_1}\right), \exp\left(-z\left(\frac{t_2}{\lambda_2}\right)^{\alpha_2}\right)\right) f_Z(z)\mathrm{d}z, \ t_1 > 0, t_2 > 0, \ i \in \{1, \ldots, n\},$$

generally lacks a closed-form expression. Consequently, joint reliability metrics must be evaluated via numerical quadrature or other approximation methods. This copula-frailty structure is especially valuable for capturing potential tail dependence that goes beyond what is explained by shared frailty alone.

A natural way to measure and interpret the strength of such dependence in reliability studies is through the Kendall tau, denoted by τ, owing to its invariance under monotonic transformations and the ease of deriving closed-form expressions in certain copula families [18]. When dependence arises purely from the gamma distributed frailty, failure times (T_{i1}, T_{i2}) of each mode are conditionally independent given Z_i, for $i \in \{1, \ldots, n\}$, and the resulting (unconditional) dependence typically increases with the frailty variance η. By contrast, our bivariate Gumbel copula with parameter $\theta \geq 1$ induces an additional conditional correlation, reflected in $\tau|Z = (\theta - 1)/\theta$. Upon integrating out Z, the overall Kendall tau depends on both η and θ, with larger values of either parameter leading to stronger observed dependence.

However, an important practical challenge arises because only the earliest failure time and its cause are typically observed in competing risks. This partial information can make it difficult to disentangle the roles of shared frailty (governed by η) and copula-based dependence (governed by θ) [42]. Additional structural assumptions or more detailed data, such as repeated failures per unit, supplementary covariates, or expert knowledge—may be needed to ensure identifiability [24,33]. In their absence, it can be inherently challenging to isolate how much of the dependence is truly due to unobserved heterogeneity rather than a direct association between the failure times of the two modes.

4 Maximum Likelihood Inference

In this section, we estimate the model parameters using the ML method and construct CIs for the reliability of dependent systems based on the ML estimation and delta methods.

4.1 Estimation

We outline parameter estimation via the ML method. Consider n independent units subject to two competing failure modes. For unit i, we observe the earliest failure time $t_i = \min_i\{T_{i1}, T_{i2}\}$ and indicators δ_{ij}, where $\delta_{ij} = 1$ if failure occurs by mode $j \in \{1, 2\}$, and $\delta_{ij} = 0$ otherwise. Consequently, if $\delta_{i1} = \delta_{i2} = 0$, the observation for unit i is right-censored. We estimate the parameter vector $\boldsymbol{\theta} = (\alpha_1, \lambda_1, \alpha_2, \lambda_2, \eta, \theta)$, where α_j and λ_j are the Weibull shape and scale parameters for mode j, η is the variance parameter of the gamma-distributed frailty, and θ is the Gumbel copula parameter capturing tail dependence.

The likelihood function for observed data $(t_i, \delta_{i1}, \delta_{i2})$, with $i \in \{1, \ldots, n\}$, is defined as

$$L(\boldsymbol{\theta}) = \prod_{i=1}^{n} f_1(t_i)^{\delta_{i1}} f_2(t_i)^{\delta_{i2}} S_{T_{i1}, T_{i2}}(t_i, t_i)^{1-(\delta_{i1}+\delta_{i2})}, \tag{2}$$

where f_j is the density for the failure time of mode j computed as $f_j(t) = -\partial/\partial t_j S_{T_{i1}, T_{i2}}(t_1, t_2)|_{t_1=t_2=t}$ for $j \in \{1, 2\}$.

Under the frailty-copula model, the joint survival function $S_{T_{i1}, T_{i2}}$ involves an integral over the gamma-distributed frailty combined with the copula. Numerical integration and differentiation techniques must be employed to evaluate the likelihood components accurately. Taking the logarithm of the function formulated in (2), we obtain the log-likelihood function $\ell(\boldsymbol{\theta})$ given by

$$\ell(\boldsymbol{\theta}) = \sum_{i=1}^{n} \left\{ \delta_{i1} \log(f_1(t_i)) + \delta_{i2} \log(f_2(t_i)) + (1 - \delta_{i1} - \delta_{i2}) \log(S_{T_{i1}, T_{i2}}(t_i, t_i)) \right\}.$$

Since $\delta_{i1} + \delta_{i2} \leq 1$, at most one density term is active per observation, and the survival function term appears only in censored observations. ML estimates are obtained numerically by solving $\widehat{\boldsymbol{\theta}} = \arg\max_{\boldsymbol{\theta}} \ell(\boldsymbol{\theta})$, typically through quasi-Newton or similar optimization algorithms. In more complex cases—particularly when both the frailty variance η and the copula parameter θ must be estimated—additional constraints or prior information may be required to ensure identifiability.

In practice, several considerations are essential to achieve robust inference. First, to avoid numerical instability or overflow, one can optimize η and θ on a logarithmic scale, guaranteeing their positivity and promoting stable convergence. Second, convergence diagnostics should include verification of gradient norms and examination of the Hessian matrix definiteness, ensuring the algorithm attains a global rather than a local maximum. Then, once the model has converged, the asymptotic covariance matrix $\boldsymbol{\Sigma}$ can be estimated by inverting the observed Fisher information matrix, that is, the negative Hessian matrix evaluated at the ML estimates. This enables the use of the delta method to construct CIs for derived reliability measures and quantiles, as described next.

4.2 Confidence Intervals for Marginal Quantiles

We now focus on constructing CIs for the marginal quantiles $t_{p,j}$, where $S_{T_j}(t_{p,j}) = 1 - p$, in the presence of a frailty-copula model, for $j \in \{1, 2\}$. Because $t_{p,j}$ is a nonlinear function of the parameter vector $\boldsymbol{\theta}$, traditional CI formulas cannot be applied directly. Instead, we use a log-transformation combined with the delta method to derive an asymptotic approximation for the quantile variance. Define the log-quantile by $y_{p,j} = \log(t_{p,j})$, for $0 < p < 1$, $j \in \{1, 2\}$, and let $\widehat{y}_{p,j}$ be its estimate obtained by plugging the ML estimate $\widehat{\boldsymbol{\theta}}$ into the marginal quantile function defined in (1). By linearizing $y_{p,j}$ around $\widehat{\boldsymbol{\theta}}$, the delta method provides an approximate standard error (SE).

Specifically, if $\widehat{\mathrm{SE}}(\widehat{y}_{p,j})$ denotes the estimated SE of $\widehat{y}_{p,j}$, then an approximate $(1 - \alpha_{\mathrm{CI}}) \times 100\%$ CI for the log-quantile is given by $[\widehat{y}_{p,j} - z_{\alpha_{\mathrm{CI}}/2}\widehat{\mathrm{SE}}(\widehat{y}_{p,j}), \widehat{y}_{p,j} + z_{\alpha_{\mathrm{CI}}/2}\widehat{\mathrm{SE}}(\widehat{y}_{p,j})]$, where $z_{\alpha_{\mathrm{CI}}/2}$ is the standard normal quantile corresponding to the chosen confidence level. Exponentiating both endpoints yields the desired interval for $t_{p,j}$, $[\exp(\underline{y}_{p,j}), \exp(\overline{y}_{p,j})]$, for $0 < p < 1$ and $j \in \{1, 2\}$.

In terms of practical implementation, evaluating $\widehat{\mathrm{SE}}(\widehat{y}_{p,j})$ requires computing the gradient of $\log(t_{p,j})$ with respect to the parameter $\boldsymbol{\theta}$. This can be done using numerical approximations (such as finite differences) or symbolic differentiation. In particular, recall that $t_{p,j}$ is implicitly defined by the equation given by $S_{T_j}(t_{p,j}; \boldsymbol{\theta}) = 1 - p$, for $0 < p < 1$ and $j \in \{1, 2\}$. Thus, differentiating this equation concerning each component of $\boldsymbol{\theta}$ allows us to track how changes in $\boldsymbol{\theta}$ propagate to $t_{p,j}$. When the model also includes copula and frailty parameters (θ, η), the corresponding derivatives must incorporate the full covariance structure $\widehat{\boldsymbol{\Sigma}}$ obtained by inverting the Fisher information matrix and evaluating it at the ML estimate (see Section 4.1).

4.3 Asymptotic Validity and Coverage

Under usual regularity conditions, ensuring that $\widehat{\boldsymbol{\theta}}$ is consistent and asymptotically normal, the log-quantile estimator $\widehat{y}_{p,j}$ converges in distribution to a normally distributed random variable centered at the true $y_{p,j} = \log(t_{p,j})$. Consequently, the resulting CIs achieve the nominal CP $1 - \alpha_{\mathrm{CI}}$ as the sample size grows. Sufficient conditions include the smoothness of $t_{p,j}(\boldsymbol{\theta})$ (so that the delta method applies) and have enough observed failures from mode $j \in \{1, 2\}$ to estimate its parameters with precision. In practice, one can further validate CP accuracy through simulation studies or bootstrap resampling.

By applying a log-transformation and the delta method, we obtain a theoretically justified procedure for constructing CIs for $t_{p,j}$. Under regularity conditions, these intervals attain the nominal CP $(1 - \alpha_{\mathrm{CI}})$ as the sample size increases.

Specifically, let S_{T_j} denote the true survival function for the failure time of mode j with quantile $t_{p,j}$, and let $\widehat{S}_{T_j}$ be the fitted counterpart derived from the ML estimate $\widehat{\boldsymbol{\theta}}$. Our CI $[\underline{t}_{p,j}, \overline{t}_{p,j}]$ must satisfy the expression formulated as

$$\Pr\left[t_{p,j} \in (\underline{t}_{p,j}, \overline{t}_{p,j})\right] = \Pr\left[\underline{y}_{p,j} \leq y_{p,j} \leq \overline{y}_{p,j}\right] \to 1 - \alpha_{\mathrm{CI}}, \quad 0 < p < 1, j \in \{1, 2\},$$

as $n \to \infty$, where $y_{p,j} = \log(t_{p,j})$ and $\underline{y}_{p,j}, \overline{y}_{p,j}$ are the log-scale bounds obtained via the delta method. For convergence to be reached, the following three main conditions are usually required:

(i) Consistency and asymptotic normality of the ML estimator distribution $\widehat{\boldsymbol{\theta}}$, which ensures a valid linear approximation of $\log(t_{p,j})$ around the true parameter values.
(ii) Smoothness of the mapping from $\boldsymbol{\theta}$ to $t_{p,j}$, so that partial derivatives exist and the gradient at the true parameter point is nonzero.
(iii) Sufficient effective sample size for each mode j, with the proportion of observed failures bounded away from zero and one, thereby guaranteeing stable estimation of both the marginal distribution and the parameter vector.

When conditions (i), (ii), and (iii) above are met, traditional asymptotic theory [33,38] implies that

$$\Pr\left[\underline{y}_{p,j} \leq y_{p,j} \leq \overline{y}_{p,j}\right] \to 1 - \alpha_{\mathrm{CI}}, \quad 0 < p < 1, j \in \{1, 2\},$$

as $n \to \infty$.

Thus, exponentiating the bounds restores a suitable CP level on the original time scale. In practice, one can further corroborate these asymptotic results via simulation studies or bootstrap resampling to assess finite-sample performance.

4.4 Implicit Differentiation and Partial Derivatives

Because $y_{p,j} = \log(t_{p,j})$ is implicitly defined as a nonlinear function of the parameter vector $\widehat{\boldsymbol{\theta}}$, we apply the delta method in conjunction with implicit differentiation to obtain $\widehat{\text{SE}}(\widehat{y}_{p,j})$. Concretely, recall that the fitted marginal survival function $\widehat{S}_{T_j}$ satisfies the relationship stated as $\widehat{S}_{T_j}(\exp(y_{p,j}); \widehat{\boldsymbol{\theta}}) = 1 - p$. Differentiating this relationship with respect to the parameters in $\widehat{\boldsymbol{\theta}}$ captures how small changes in $\widehat{\boldsymbol{\theta}}$ propagate to $y_{p,j}$. To organize these effects, let

$$\Delta_{1,j} = \frac{\partial \widehat{S}_{T_j}(\exp(y_{p,j}))}{\partial y_{p,j}} = -f_j(\exp(y_{p,j})) \exp(y_{p,j}), \quad 0 < p < 1, j \in \{1,2\}, \tag{3}$$

where f_j is the fitted marginal density of the failure time for mode j. The partial derivative presented in (3) tracks the sensitivity of $\widehat{S}_{T_j}$ to infinitesimal shifts in $y_{p,j}$. In parallel, let

$$\Delta_{2,j}^2 = \frac{\partial \exp(y_{p,j})}{\partial \widehat{\boldsymbol{\theta}}}^{\top} \widehat{\boldsymbol{\Sigma}} \frac{\partial \exp(y_{p,j})}{\partial \widehat{\boldsymbol{\theta}}}, \quad 0 < p < 1, j \in \{1,2\}, \tag{4}$$

where $\widehat{\boldsymbol{\Sigma}}$ is the asymptotic covariance matrix (obtained from the inverse observed Fisher information at $\widehat{\boldsymbol{\theta}}$), and $\partial \exp(y_{p,j})/\partial \widehat{\boldsymbol{\theta}}$ is the gradient vector of $\exp(y_{p,j})$ with respect to $\widehat{\boldsymbol{\theta}}$. The two partial derivatives presented in (3) and (4) combine to yield

$$\widehat{\text{SE}}(\widehat{y}_{p,j}) = \frac{\sqrt{\Delta_{2,j}^2}}{|\Delta_{1,j}|}, \quad 0 < p < 1, j \in \{1,2\}.$$

Under usual regularity assumptions, including the consistency and asymptotic normality of $\widehat{\boldsymbol{\theta}}$, we have $\widehat{\text{SE}}(\widehat{y}_{p,j}) \xrightarrow{\mathcal{P}} 0$ as $n_j \to \infty$, which ensures that the delta-method-based CIs for $t_{p,j}$ converge to the correct nominal CP, where $\xrightarrow{\mathcal{P}}$ means convergence in probability to.

4.5 Taylor Expansions and Coverage Probability

To further elucidate why the proposed CIs converge to the nominal level, we use a Taylor expansion of the estimated marginal survival function $\widehat{S}_{T_j}$ around the true log-quantile $y_{p,j} = \log(t_{p,j})$. Define a small shift by means of $\widetilde{y}_{p,j} = y_{p,j} + z_{1-\alpha_{\text{CI}}/2} \Delta_{2,j}/|\Delta_{1,j}|$, where $\Delta_{1,j}$ and $\Delta_{2,j}$ are defined in (3) and (4), respectively, for $0 < p < 1$ and $j \in \{1,2\}$.

By expanding $\widehat{S}_{T_j}(\exp(\widetilde{y}_{p,j}))$ around $y_{p,j}$, we get

$$\widehat{S}_{T_j}(\exp(\widetilde{y}_{p,j})) \approx \widehat{S}_{T_j}(\exp(y_{p,j})) + \frac{\partial \widehat{S}_{T_j}(\exp(y_{p,j}))}{\partial y_{p,j}} \left(z_{1-\alpha_{\text{CI}}/2} \frac{\Delta_{2,j}}{|\Delta_{1,j}|}\right) + R_{n,j}, \quad 0 < p < 1, j \in \{1,2\},$$

where $R_{n,j} = o_p(1)$, that is, the order of approximation. Since $\widehat{S}_{T_j}(\exp(y_{p,j})) \approx S_{T_j}(t_{p,j}) = 1 - p$, and recalling $\Delta_{1,j} < 0$, the shift in $\widehat{S}_{T_j}$ is approximately given by $(1 - p) - z_{1-\alpha_{\text{CI}}/2} \Delta_{2,j} + R_{n,j}$.

An analogous argument applies to the lower bound $\underline{y}_{p,j}$. Hence, the event $\{\widehat{S}_{T_j}(\exp(\widetilde{y}_{p,j})) \leq (1-p) \leq \widehat{S}_{T_j}(\exp(\underline{y}_{p,j}))\}$ translates into a statement about the standardized difference $(\widehat{S}_{T_j}(t_{p,j}) - S_{T_j}(t_{p,j}))/\Delta_{2,j}$, which converges in distribution to a normal distributed standard random variable by the delta method and the asymptotic normality of the distribution for $\widehat{\boldsymbol{\theta}}$. As the sample size n_j (the effective sample size for mode j) becomes large, this probability approaches $1 - \alpha_{\mathrm{CI}}$.

4.6 Asymptotic Normality and Slutsky Theorem

Under regularity conditions ensuring that $\widehat{\boldsymbol{\theta}}$ is both consistent and asymptotically normal distributed, the random variable is defined as $(\widehat{S}_{T_j}(t_{p,j}) - S_{T_j}(t_{p,j}))/\Delta_{2,j} \xrightarrow{\mathcal{D}} \mathrm{Normal}(0,1)$, for $0 < p < 1$ and $j \in \{1, 2\}$, where $\xrightarrow{\mathcal{D}}$ means convergence in distribution to. Moreover, the remainder terms in the Taylor expansion vanish as $n_j \to \infty$. The Slutsky theorem guarantees that the true CP converges to $1 - \alpha_{\mathrm{CI}}$. Consequently, the log-transformed delta-method CI for $t_{p,j}$ attains the nominal CP as the sample grows.

In summary, the asymptotic validity of our interval estimators for $t_{p,j}$ follows from a combination of (i) implicit differentiation of the quantile definition, (ii) taylor expansions around the true log-quantile, and (iii) traditional asymptotic results on ML estimators, culminating in a robust procedure for quantifying uncertainty in marginal quantiles under dependent competing risks.

5 Simulation Study

This section describes a simulation study aimed at evaluating our proposed CIs for the reliability of a two-component series system, where component lifetimes follow Weibull distributions with a gamma-distributed frailty and are linked by a Gumbel copula. We assess the CPs of these CIs under different dependence levels (quantified by Kendall's tau, τ) and various censoring rates. We further compare our adjusted intervals with two traditional approaches and examine how the sample size affects the mean time to failure (MTTF).

5.1 Setup and Frailty-Dependence Modeling

We adopt a gamma-distributed frailty Z to capture unobserved heterogeneity among units, governed by the variance parameter η. As η approaches zero, the frailty collapses to $Z = 1$ (no extra heterogeneity). Larger values of η imply stronger unobserved heterogeneity, typically increasing the marginal correlation of failure times. Conditionally on $Z = z$, each component follows a Weibull distribution with shape α_j and scale λ_j, for $j \in \{1, 2\}$. Beyond the shared frailty, a Gumbel copula (parameterized by $\theta \geq 1$) introduces additional tail dependence. This setup accommodates both latent heterogeneity (via η) and direct association (via θ).

5.2 Implementation and Comparison of Interval Methods

For each generated dataset of size n, we estimate the parameter vector $\boldsymbol{\theta} = (\alpha_1, \lambda_1, \alpha_2, \lambda_2, \eta, \theta)$ by maximizing the full log-likelihood function introduced in Section 3. As there is a closed-form for the integral over the gamma frailty or the partial derivatives of the copula-based survival function, we rely on numerical integration combined with finite-difference approximations as follows:

- We use `integrate()` (the base R adaptive quadrature routine) or simple Monte Carlo methods to evaluate the integrals over the gamma frailty distribution.
- We employ `numDeriv` for finite-difference approximations of partial derivatives, which are needed to compute $f_j(t)$ in the likelihood.

- We call `optim()` (BFGS or L-BFGS-B) for quasi-Newton optimization, facilitating parameter constraints (such as positivity of η, θ) and promoting stable convergence.

Following the expression stated in (2), each observation $(t_i, \delta_{i1}, \delta_{i2})$ contributes a density term $f_j(t_i)$ if $\delta_{ij} = 1$, or a survival term $S_{T_{i1}, T_{i2}}(t_i, t_i)$ if the observation is censored. To avoid numerical under-/overflow and to ensure positivity (or boundedness) of parameters, we often reparametrize η and θ on a log-scale. For instance, if θ must satisfy $\theta \geq 1$, we let $\theta^* \in \mathbb{R}$ and define $\theta = 1 + \exp(\theta^*)$, where θ^* is the unconstrained parameter manipulated by the optimizer, guaranteeing that $\theta \geq 1$. Convergence is monitored by checking the gradient norm and the definiteness of the Hessian matrix. If the Hessian matrix is nearly singular –for instance, due to strong dependence or small sample sizes– we optionally add a mild ridge penalty to stabilize the fit.

5.3 Coverage Probability

We adopt the procedure outlined in Algorithm 1 to obtain empirical CPs for the proposed CI methods. In each simulation replicate, we generate a latent gamma distributed frailty $Z_i \sim \Gamma(1/\eta, \eta)$, use a Gumbel copula (parameter θ) to introduce dependence among the Weibull-distributed times, and optionally impose right-censoring.

After generating $(t_{\text{obs},i}, \delta_{i1}, \delta_{i2})$ for each unit, we compute the log-likelihood function, substituting $f_j(t) = -\partial/\partial t_j S_{T_{i1}, T_{i2}}(t_1, t_2)|_{t_1=t_2=t}$ into the expression stated as (2), and maximize it via quasi-Newton routines. Once $\widehat{\theta}$ is obtained, we invert the observed Fisher information to estimate the covariance matrix. A log-transform delta method then provides CIs for marginal quantiles $t_{p,j}$ (see Section 4 for details).

Algorithm 1: Monte carlo simulation procedure

Input:

　N_{rep}: number of replicates

　n: sample size

　Parameters $(\alpha_1, \alpha_2, \lambda_1, \lambda_2, \eta, \theta)$

　Optional censoring rate or times $\{C_i\}$, for $i \in \{1, \ldots, n\}$

　for $r = 1$ to N_{rep} **do**

　　Step 1: Generate the data

　　1.1 Generate a gamma distributed frailty $Z_i \sim \Gamma(1/\eta, \eta)$ for $i \in \{1, \ldots, n\}$.

　　1.2 Condition on $Z_i = z$ and sample (T_{i1}, T_{i2}) (Weibull) with copula Gumbel(θ).

　　1.3 Compute $T_{\text{obs},i} = \min\{T_{i1}, T_{i2}\}$.

　　1.4 Determine δ_{i1}, δ_{i2} accordingly, applying right-censoring if desired.

　　Step 2: Evaluate the log-likelihood function

　　2.1 Numerically integrate over Z_i to obtain $S_{T_{i1}, T_{i2}}(t, t)$.

　　2.2 Approximate derivatives to get $f_j(t)$.

　　2.3 Substitute in the expression stated as (2) to form the likelihood function.

　　Step 3: Estimate the parameters

　　3.1 Maximize the negative log-likelihood function (`optim` with BFGS).

　　3.2 Reparameterize $\lambda_j = \exp(\phi_j)$, $\eta = \exp(\phi_\eta)$, $\theta = 1 + \exp(\phi_\theta)$.

　　3.3 Add mild ridge penalty if Hessian matrix is near-singular,

　　3.4 Check convergence and definiteness of the Hessian matrix.

(Continued)

Algorithm 1 (continued)

   Step 4: Construct confidence intervals

  4.1 Invert the observed Fisher information to get $\widehat{\Sigma}$.

  4.2 Apply a log-delta method for each marginal quantile $t_{p,j}$.

  4.3 Obtain $\mathrm{CI_{Dep}}, \mathrm{CI_{ML}}, \mathrm{CI_{Logit}}$.

   Step 5: Coverage Probability Computation

  5.1 *Record* whether each true value lies inside the computed CIs.

  5.2 *Calculate* the empirical coverage probability (CP) as the fraction of replicates covering the true

parameter or quantile.

  end for

Output:

  Empirical CPs for each CI method.

Following the steps in Algorithm 1, we evaluate the CP for each triple $(n, \theta, \texttt{censoring\_rate})$, where n is the sample size, $\theta \geq 1$ is the Gumbel copula parameter controlling the dependence strength, and $\texttt{censoring\_rate}$ is the rate parameter for exponential censoring times $\{C_i\}$. We construct the proposed $\mathrm{CI_{Dep}}$, along with the simple $\mathrm{CI_{ML}}$ and $\mathrm{CI_{Logit}}$, all at the nominal 95% confidence level. The R code in Appendix 1 focuses on $\mathrm{CI_{Dep}}$. We then summarize the resulting CPs for each combination of sample size, dependence level, and censoring scenario in the tables below.

5.4 Dependence Levels and Scenarios without Censoring

We examine three levels of dependence for Weibull-distributed failure times: weak, moderate, and strong. These are measured via the conditional Kendall's tau, denoted by $\tau_{\theta|Z}$, which quantifies the correlation between the two components given the latent frailty Z. Concretely, we set: $\tau_{\theta|Z} = 0.25$ (weak), $\tau_{\theta|Z} = 0.50$ (moderate), and $\tau_{\theta|Z} = 0.75$ (strong). Throughout this article, we use a Gumbel copula with parameter $\theta \geq 1$. In this copula, the conditional Kendall's tau is given by $\tau_{\theta|Z} = 1 - 1/\theta$. Hence, for example, $\tau_{\theta|Z} = 0.25$ implies $\theta \approx 1.33$, $\tau_{\theta|Z} = 0.50$ implies $\theta = 2$, and $\tau_{\theta|Z} = 0.75$ implies $\theta = 4$. Together with the Weibull parameters $\alpha_1, \alpha_2, \lambda_1, \lambda_2$ and the frailty variance η, these values define the data-generating processes in all of our simulations.

5.5 Simulations with Complete Data (No Censoring)

To first isolate the effect of dependence on coverage, we consider the no-censoring case (0%). Tables 2–4 show the estimated 95% CPs for various sample sizes and quantiles p. Each table compares the following:

- $\mathrm{CI_{ML}}$—The method from [39], assuming independence,
- $\mathrm{CI_{Logit}}$—Logit-transform CIs without accounting for the copula,
- $\mathrm{CI_{Dep}}$—Our adjusted approach that includes both η and θ in its variance structure.

Fig. 1 summarizes the simulation design. Subsequent sections present analogous CP results under 10% and 25% censoring to represent more realistic scenarios with partially observed lifetimes.

For the case of weak dependence, $\tau_{\theta|Z} = 0.25$, Table 2 shows that all methods produce CPs close to the nominal 95%, even for small sample sizes. At $n = 50$, there are slight deviations below 0.95 for some intervals, but overall, the differences between the traditional CIs [39], the logit-based CIs, and our proposed adjusted intervals are modest. As n increases, CP across all methods quickly stabilizes near the nominal level, with the adjusted intervals often exhibiting slightly better stability at certain quantiles.

Table 2: CPs for 95% CIs under weak dependence ($\tau_{\theta|Z} = 0.25$; $\theta \approx 1.33$) with no censoring, across methods and sample sizes

n	p	CI_{Dep}	CI_{ML}	CI_{Logit}	n	p	CI_{Dep}	CI_{ML}	CI_{Logit}
50	0.05	0.943	0.950	0.942	100	0.05	0.946	0.950	0.944
	0.25	0.945	0.950	0.942		0.25	0.947	0.950	0.946
	0.50	0.945	0.950	0.943		0.50	0.949	0.950	0.946
	0.75	0.949	0.950	0.945		0.75	0.950	0.950	0.947
	0.95	0.949	0.950	0.946		0.95	0.949	0.950	0.948
500	0.05	0.948	0.950	0.947	1000	0.05	0.949	0.950	0.948
	0.25	0.949	0.950	0.946		0.25	0.950	0.950	0.950
	0.50	0.949	0.950	0.948		0.50	0.950	0.950	0.949
	0.75	0.950	0.950	0.948		0.75	0.949	0.950	0.950
	0.95	0.950	0.950	0.950		0.95	0.949	0.950	0.949

Table 3: CPs for 95% CIs under moderate dependence ($\tau_{\theta|Z} = 0.50$; $\theta = 2$) with no censoring, across methods and sample sizes

n	p	CI_{Dep}	CI_{ML}	CI_{Logit}	n	p	CI_{Dep}	CI_{ML}	CI_{Logit}
50	0.05	0.945	0.950	0.933	100	0.05	0.946	0.950	0.943
	0.25	0.945	0.950	0.936		0.25	0.946	0.950	0.940
	0.50	0.946	0.950	0.942		0.50	0.948	0.950	0.945
	0.75	0.946	0.950	0.946		0.75	0.948	0.950	0.947
	0.95	0.948	0.950	0.947		0.95	0.949	0.950	0.948
500	0.05	0.948	0.950	0.946	1000	0.05	0.949	0.950	0.948
	0.25	0.948	0.950	0.946		0.25	0.949	0.950	0.947
	0.50	0.949	0.950	0.947		0.50	0.950	0.950	0.949
	0.75	0.950	0.950	0.948		0.75	0.950	0.950	0.950
	0.95	0.950	0.950	0.948		0.95	0.949	0.950	0.950

Table 4: CPs for 95% CIs under strong dependence ($\tau_{\theta|Z} = 0.75$; $\theta = 4$) with no censoring, across methods and sample sizes

n	p	CI_{Dep}	CI_{ML}	CI_{Logit}	n	p	CI_{Dep}	CI_{ML}	CI_{Logit}
50	0.05	0.944	0.950	0.928	100	0.05	0.946	0.950	0.940
	0.25	0.945	0.950	0.929		0.25	0.946	0.950	0.940
	0.50	0.945	0.950	0.937		0.50	0.947	0.950	0.942
	0.75	0.946	0.950	0.940		0.75	0.947	0.950	0.937
	0.95	0.947	0.950	0.940		0.95	0.948	0.950	0.938
500	0.05	0.948	0.950	0.946	1000	0.05	0.949	0.950	0.946
	0.25	0.948	0.950	0.945		0.25	0.949	0.950	0.947
	0.50	0.950	0.950	0.945		0.50	0.949	0.950	0.946
	0.75	0.950	0.950	0.948		0.75	0.949	0.950	0.946
	0.95	0.949	0.950	0.945		0.95	0.949	0.950	0.947
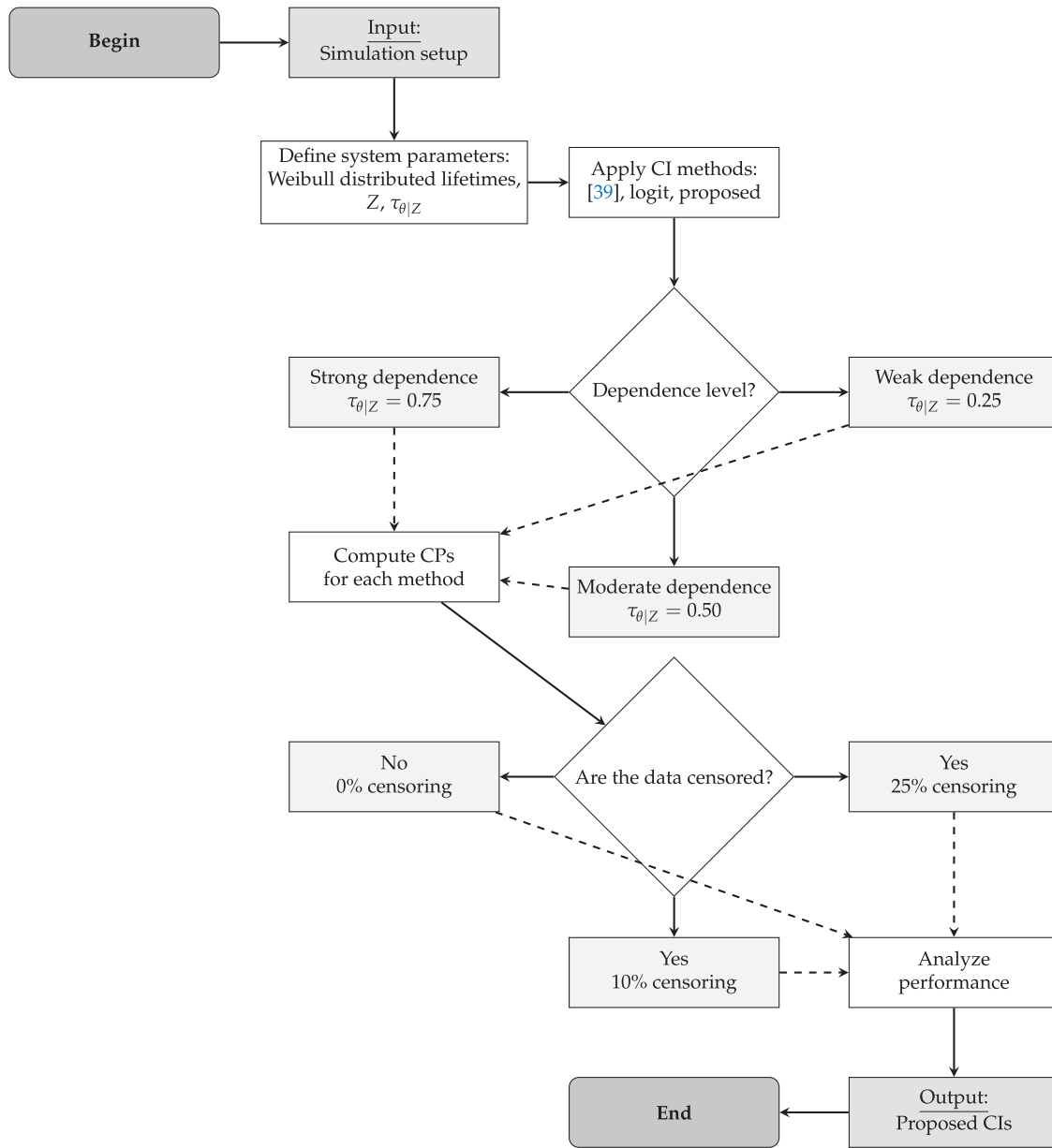
Figure 1: Flowchart of the simulation process for evaluating the impact of frailty on system reliability [39]

In the case of moderate dependence, $\tau_{\theta|Z} = 0.50$, as reported in Table 3, the CPs again remain fairly close to 95%, although small-sample settings ($n = 50$) display mild fluctuations around the nominal target. The traditional CIs [39] and logit-based CIs are generally in line with the adjusted intervals, and any under- or over-coverage tends to be within a few percentage points. As before, increasing the sample size mitigates these minor deviations.

Under strong dependence, $\tau_{\theta|Z} = 0.75$ (see Table 4), the CPs continue to cluster around the nominal 95%. Although minor under- or over-coverage can appear for very small n, the magnitude of such deviations is not large. The adjusted intervals do show somewhat steadier performance across sample sizes in these high-dependence scenarios, but the traditional and logit-based CIs remain reasonably accurate as well.

Overall, sample size still plays a role in CP performance, with all methods converging toward the nominal 95% as n grows (such as at $n = 500$ or $n = 1000$). The corrected intervals tend to be slightly more robust under stronger dependence or smaller n, but the numerical differences between the traditional and logit-based CIs are generally modest. These differences demonstrate that incorporating both the frailty variance η and the copula parameter θ can offer a small edge in maintaining nominal CP, particularly in more challenging settings.

5.6 Effect of Censoring on Confidence Interval Coverage

We now evaluate how additional right-censoring affects CPs under the same configurations stated in Section 5.4. Specifically, we apply 10% and 25% censoring and report results in Tables 5–7 (for 10%) and Tables 8–10 (for 25%).

Table 5: CPs for 95% CIs under weak dependence ($\tau_{\theta|Z} = 0.25$; $\theta \approx 1.33$) with a 10% censoring rate. Columns show sample size n, quantile p, and CPs for CI_{Dep}, CI_{ML}, and CI_{Logit}

n	p	CI_{Dep}	CI_{ML}	CI_{Logit}	n	p	CI_{Dep}	CI_{ML}	CI_{Logit}
50	0.05	0.945	0.950	0.939	100	0.05	0.945	0.950	0.943
	0.25	0.947	0.950	0.939		0.25	0.945	0.950	0.943
	0.50	0.946	0.950	0.945		0.50	0.946	0.950	0.944
	0.75	0.946	0.950	0.947		0.75	0.947	0.950	0.947
	0.95	0.949	0.950	0.948		0.95	0.949	0.950	0.945
500	0.05	0.947	0.950	0.945	1000	0.05	0.948	0.950	0.949
	0.25	0.947	0.950	0.945		0.25	0.949	0.950	0.949
	0.50	0.949	0.950	0.946		0.50	0.950	0.950	0.949
	0.75	0.949	0.950	0.947		0.75	0.950	0.950	0.949
	0.95	0.950	0.950	0.947		0.95	0.950	0.950	0.950

Table 6: CPs for 95% CIs under moderate dependence $\tau_{\theta|Z} = 0.50$ and a 10% censoring rate with the indicated method

n	p	CI_{Dep}	CI_{ML}	CI_{Logit}	n	p	CI_{Dep}	CI_{ML}	CI_{Logit}
50	0.05	0.943	0.950	0.941	100	0.05	0.945	0.950	0.945
	0.25	0.946	0.950	0.941		0.25	0.948	0.950	0.944
	0.50	0.944	0.950	0.944		0.50	0.948	0.950	0.945
	0.75	0.943	0.950	0.943		0.75	0.947	0.950	0.946
	0.95	0.947	0.950	0.944		0.95	0.947	0.950	0.947
500	0.05	0.946	0.950	0.946	1000	0.05	0.949	0.950	0.947
	0.25	0.947	0.950	0.950		0.25	0.948	0.950	0.949
	0.50	0.946	0.950	0.948		0.50	0.950	0.950	0.948
	0.75	0.950	0.950	0.947		0.75	0.950	0.950	0.950
	0.95	0.949	0.950	0.948		0.95	0.949	0.950	0.950

Table 7: CPs for 95% CIs under strong dependence $\tau_{\theta|Z} = 0.75$ and a 10% censoring rate

n	p	CI_{Dep}	CI_{ML}	CI_{Logit}	n	p	CI_{Dep}	CI_{ML}	CI_{Logit}
50	0.05	0.935	0.950	0.932	100	0.05	0.941	0.950	0.945
	0.25	0.936	0.950	0.932		0.25	0.942	0.950	0.940
	0.50	0.939	0.950	0.938		0.50	0.945	0.950	0.939
	0.75	0.940	0.950	0.940		0.75	0.941	0.950	0.940
	0.95	0.936	0.950	0.939		0.95	0.940	0.950	0.939
500	0.05	0.940	0.950	0.940	1000	0.05	0.948	0.950	0.948
	0.25	0.941	0.950	0.940		0.25	0.949	0.950	0.948
	0.50	0.943	0.950	0.940		0.50	0.948	0.950	0.950
	0.75	0.945	0.950	0.945		0.75	0.949	0.950	0.947
	0.95	0.945	0.950	0.943		0.95	0.950	0.950	0.948

Table 8: CPs for 95% CIs under weak dependence ($\tau_{\theta|Z} = 0.25$) and a 25% censoring rate with the indicated method

n	p	CI_{Dep}	CI_{ML}	CI_{Logit}	n	p	CI_{Dep}	CI_{ML}	CI_{Logit}
50	0.05	0.938	0.950	0.933	100	0.05	0.940	0.950	0.940
	0.25	0.940	0.950	0.934		0.25	0.939	0.950	0.939
	0.50	0.940	0.950	0.935		0.50	0.940	0.950	0.940
	0.75	0.937	0.950	0.936		0.75	0.940	0.950	0.941
	0.95	0.939	0.950	0.940		0.95	0.939	0.950	0.940
500	0.05	0.945	0.950	0.945	1000	0.05	0.948	0.950	0.947
	0.25	0.945	0.950	0.944		0.25	0.945	0.950	0.948
	0.50	0.945	0.950	0.944		0.50	0.945	0.950	0.948
	0.75	0.944	0.950	0.944		0.75	0.949	0.950	0.947
	0.95	0.947	0.950	0.945		0.95	0.948	0.950	0.949

Under 10% censoring, CPs for smaller samples ($n = 50$) decrease slightly for all methods, particularly at lower quantiles ($p = 0.05$), but remain close to 95%. The traditional CIs [39] and logit-based CIs occasionally dip a bit below nominal CP with moderate or strong dependence, whereas the corrected intervals tend to stay near 95% even at $n = 50$. As the sample size grows, differences among the methods generally diminish.

Moving to 25% censoring amplifies these differences somewhat, especially with strong dependence ($\tau_{\theta|Z} = 0.75$) and small n. In such cases, the traditional CIs [39] and logit-based CIs show slightly lower CP, but typically not drastically below 95%. Meanwhile, the corrected CIs maintain CPs closer to the nominal level across the quantiles reported. As n increases beyond 100, the gap again narrows, and all methods converge to near 95%.

In summary, whether censoring is present or not, the adjusted CIs consistently provide CPs near the nominal level, especially in higher-dependence regimes and smaller sample sizes, where even slight improvements can be valuable. Hence, incorporating both the copula parameter θ and the frailty variance η in the variance-covariance structure offers practical benefits for reliability analyses involving censoring and interdependent component failure times.

Table 9: CPs for 95% CIs under moderate dependence ($\tau_{\theta|Z} = 0.50$) and a 25% censoring rate with the indicated method

n	p	$\mathbf{CI_{Dep}}$	$\mathbf{CI_{ML}}$	$\mathbf{CI_{Logit}}$	n	p	$\mathbf{CI_{Dep}}$	$\mathbf{CI_{ML}}$	$\mathbf{CI_{Logit}}$
50	0.05	0.935	0.950	0.940	100	0.05	0.942	0.950	0.942
	0.25	0.932	0.950	0.938		0.25	0.944	0.950	0.944
	0.50	0.933	0.950	0.940		0.50	0.944	0.950	0.942
	0.75	0.932	0.950	0.941		0.75	0.945	0.950	0.944
	0.95	0.934	0.950	0.940		0.95	0.945	0.950	0.945
500	0.05	0.945	0.950	0.946	1000	0.05	0.948	0.950	0.946
	0.25	0.947	0.950	0.948		0.25	0.948	0.950	0.947
	0.50	0.946	0.950	0.948		0.50	0.948	0.950	0.948
	0.75	0.948	0.950	0.948		0.75	0.948	0.950	0.948
	0.95	0.947	0.950	0.949		0.95	0.949	0.950	0.948

Table 10: CPs for 95% CIs under strong dependence ($\tau_{\theta|Z} = 0.75$) and a 25% censoring rate with the indicated method

n	p	$\mathbf{CI_{Dep}}$	$\mathbf{CI_{ML}}$	$\mathbf{CI_{Logit}}$	n	p	$\mathbf{CI_{Dep}}$	$\mathbf{CI_{ML}}$	$\mathbf{CI_{Logit}}$
50	0.05	0.932	0.950	0.934	100	0.05	0.938	0.950	0.939
	0.25	0.934	0.950	0.933		0.25	0.937	0.950	0.938
	0.50	0.935	0.950	0.934		0.50	0.938	0.950	0.938
	0.75	0.939	0.950	0.940		0.75	0.939	0.950	0.940
	0.95	0.938	0.950	0.938		0.95	0.940	0.950	0.938
500	0.05	0.942	0.950	0.941	1000	0.05	0.947	0.950	0.946
	0.25	0.940	0.950	0.941		0.25	0.948	0.950	0.947
	0.50	0.942	0.950	0.941		0.50	0.949	0.950	0.949
	0.75	0.946	0.950	0.944		0.75	0.946	0.950	0.946
	0.95	0.944	0.950	0.945		0.95	0.949	0.950	0.947

5.7 Impact of Dependence and Heterogeneity on System Reliability

Next, we investigate how varying the dependence among Weibull-distributed failure times affects both the system reliability and the mean time to failure (MTTF) in a two-component series system. Specifically, we adopt a Gumbel copula parameterized by $\theta \geq 1$, where Kendall's tau is given by $\tau = 1 - 1/\theta$. Thus, as θ grows, the positive dependence among components becomes stronger. Concretely, we consider dependence levels ranging from $\tau = 0.167$ (weak) up to $\tau = 0.800$ (very strong). For instance, $\tau = 0.167$ corresponds to $\theta \approx 1.2$, whereas $\tau = 0.800$ corresponds to $\theta \approx 5.0$. We simulate 10,000 independent realizations for each τ value, aiming to observe how higher correlation influences both the reliability at a specified time horizon and the MTTF under strong dependence scenarios.

Table 11 summarizes our main results for reliability and MTTF, together with their bootstrap CIs. As expected for a series configuration, increasing dependence leads to lower reliability. Indeed, when τ grows from 0.167 to 0.800, the estimated reliability (at a given time) declines considerably. Likewise, the MTTF decreases, indicating that a higher degree of correlation among component failures makes it more likely that both components fail at earlier times.

Table 11: Numerical results for system reliability and MTTF (with bootstrap CIs) under different levels of Gumbel copula dependence. Higher τ implies stronger positive dependence

θ	τ	Reliability	MTTF	Reliability CI (lower)	Reliability CI (upper)	MTTF CI (lower)	MTTF CI (upper)
1.2	0.167	0.071	8.38	0.066	0.076	8.19	8.56
1.5	0.333	0.046	6.97	0.042	0.051	6.82	7.12
2.0	0.500	0.019	5.00	0.017	0.022	4.90	5.10
3.0	0.667	0.0028	2.58	0.0018	0.0038	2.53	2.64
4.0	0.750	0.0003	1.33	0.0000	0.00064	1.30	1.36
5.0	0.800	0.0003	0.67	0.0000	0.00064	0.66	0.69

As τ intensifies, both the reliability (at the chosen time) and the MTTF show a marked decrease, which is precisely what one expects in a series system: if one component fails prematurely and the other is highly correlated, both are likely to fail in close succession, thereby shortening the overall system lifetime. The bootstrap CIs also become narrower at higher τ in these simulations, reflecting increased homogeneity when both components tend to fail together.

Overall, these findings highlight the importance of accurately modeling dependence in series systems. Greater positive dependence (higher θ, thus higher τ) substantially lowers reliability and MTTF, consistent with theoretical expectations. We note that, while simpler methods ignoring dependence can underestimate the risk of early failure, our copula-frailty framework more realistically captures correlated failures, underscoring its relevance for reliability studies of high-dependence scenarios.

Future research may consider more complex or higher-dimensional dependence structures (such as multi-component series systems), as well as various censoring schemes, to further assess the stability of reliability estimation in strongly interdependent environments.

6 Illustrative Example with Penalized Estimation

In this section, we illustrate the practical implications of our method by conducting a synthetic case study designed to mimic a challenging real-world scenario. Specifically, we show how strong dependence, small samples, and estimation under a penalized likelihood framework can lead to non-trivial outcomes in practice. Here, we complement our previous discussion (see Section 5.7) on how dependence affects the system reliability and MTTF.

6.1 Rationale and Study Design

We consider a system of two-components connected in series for which each component time-to-failure follows a Weibull distribution (here taken as an exponential for simplicity), conditional on a gamma distributed frailty Z_i. Dependence between the two failure times is introduced via a Gumbel copula with parameter θ, while the variance parameter of the frailty is η. To explore a hard-to-estimate case, we nominally set the values given by $\lambda_1 = 40$, $\lambda_2 = 20$, $\eta = 0.3$, $\theta = 2.0$, and hence $\tau = 1 - 1/2 = 0.50$, which would typically generate relatively rare failures (owing to large λ_j) and moderately strong dependence. Then, we simulate $n = 3000$ observations, but, in practice, the data can deviate substantially from these nominal parameters, such as many failures might occur much earlier than anticipated. Also, we introduce a moderate censoring mechanism by drawing censored times from an exponential distribution with rate (mean) ≈ 0.001. Although this is intended to be a friendly censoring scheme, the real data can still pose considerable challenges if unusually early failures dominate.

6.2 Penalized Likelihood Function

As discussed in Section 4.1, ML estimation may suffer a degenerate Hessian matrix if the data exhibit strong dependence or the sample contains insufficient information to separate the copula and frailty parameters. To mitigate this degeneracy, we adopt a ridge-type penalization approach [39], adding a term $\alpha \sum_k (\theta_k - m_k)^2$ to the negative LL function, where $\alpha > 0$ is a small penalty coefficient, and $(\theta_k - m_k)$ represents the deviation of a log-parameter from some center m_k. This penalty injects additional curvature in near-flat directions, thereby helping to produce a non-singular Hessian matrix so that SEs and CIs can be computed.

6.3 Results and Observations

Fig. 2 sketches the simulation and estimation process. In one representative synthetic dataset, consider the following:

- We nominally set $(\lambda_1, \lambda_2, \eta, \theta) = (40, 20, 0.3, 2)$.
- The data, however, had a far larger proportion of early failures than expected, with a definitive cause distribution of roughly $(0.4\%, 35.0\%, 64.6\%)$ for {censored, cause 1, cause 2}. Such a proportion of short failure times can starkly contradict initial assumptions.
- Fitting via the ML estimate without penalization yielded a nearly singular Hessian matrix, preventing computation SEs and CIs.
- After imposing a moderate ridge penalty ($\alpha = 0.1$), the Hessian matrix became invertible. Our definitive estimates were $\widehat{\lambda}_1 \approx 1.03$, $\widehat{\lambda}_2 \approx 1.10$, $\widehat{\eta} \approx 1.02$, and $\widehat{\theta} \approx 2.01$. Although they deviate substantially from the nominal values, we were able to quantify large uncertainty (SEs of about ± 2 on the log-scale), resulting in feasible albeit broad CIs.
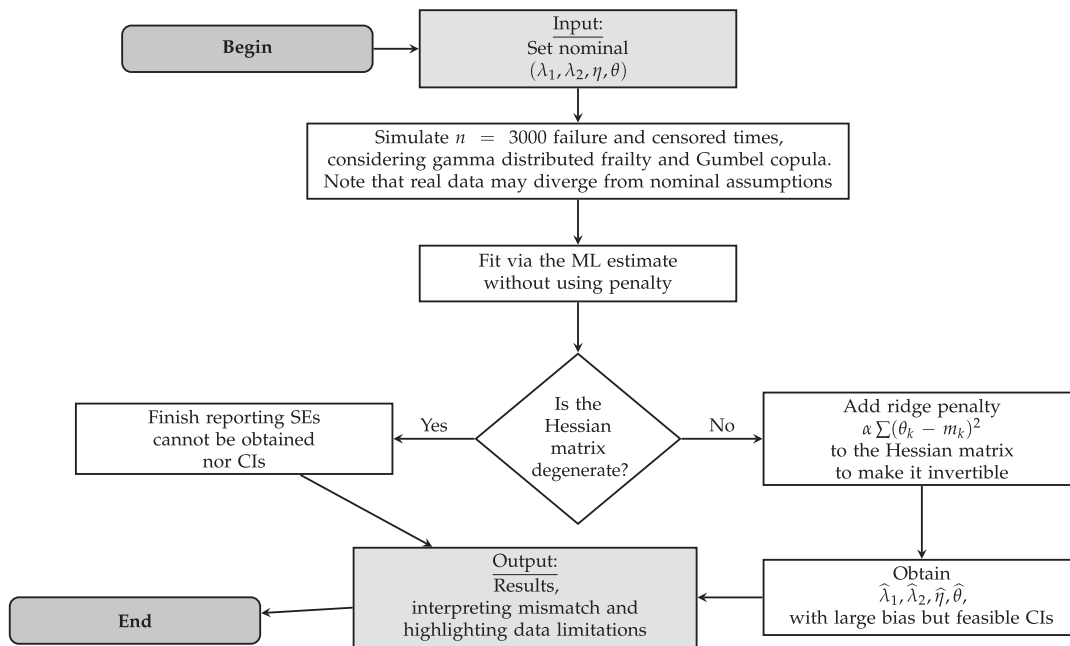
Figure 2: Flowchart illustrating penalized estimation in the challenging-data scenario. Without a penalty, the Hessian matrix may degenerate preventing SE computation. Adding a ridge penalty $\alpha > 0$ ensures an invertible Hessian matrix but can introduce bias. Either outcome signals that the data deviate substantially from nominal assumptions

6.4 Interpretation, Relevance, and Role of α

Although the definitive estimates deviate sharply from $(40, 20, 0.3, 2)$, these estimates highlight a realistic challenge: if the observed data differ markedly from initial assumptions, naive ML struggles to fit a multi-parameter frailty-copula model. Penalization enforces added curvature, preventing Hessian matrix degeneracy and enabling valid inference. However, the strength of α strongly influences the result such as indicated as follows:

- Large values of α can stabilize the estimation by shrinking parameter estimates toward nominal centers, often yielding small SEs but potentially larger bias.
- Small values of α give the data more weight but can cause near-singular Hessian matrices if the information is insufficient to separate frailty and copula effects, leading to extremely large uncertainties or unstable estimates.

In a genuine industrial or engineering scenario, such results might appear if a system nominally expected to exhibit few failures (large λ_j) instead of experiencing multiple early failures due to unforeseen stressors. Our penalized approach can at least provide the following:

- Finite SEs to gauge how severely the data deviate from the nominal scenario.
- A strong signal that model assumptions may be misaligned (as evidenced by substantial parameter shifts and wide CIs).

Hence, from a reliability engineering viewpoint, even sophisticated models can become unstable if the data are insufficient or unrepresentative. Thus, incorporating penalization or prior knowledge helps to ensure a basic level of inferential robustness.

6.5 Link to Real Applications

Although we do not present a real industrial dataset, this synthetic, real-like example is crafted to reflect high dependence and limited effective sample information. Practitioners commonly face similarly uncooperative data (sparse, heavily censored, or dominated by unanticipated early failures). Our penalized estimation strategy (frailty + copula + ridge) maintains a non-degenerate Hessian matrix, yielding SEs and CIs at the cost of potential bias. In realistic contexts, engineers may combine these estimates with domain expertise, covariate adjustments, or additional reliability testing to ease identifiability concerns. Overall, this synthetic, real-like study underlines the importance of robust or penalized approaches under strong dependence and sparse data. They avert numerical degeneracies and elucidate the degree of uncertainty, even if the ultimate parameter estimates deviate profoundly from nominal values.

7 Conclusions

In this article, we developed confidence intervals for dependent failure times in a two-component system, using Weibull distributed failure times combined with gamma distributed frailty and copula-based dependence. By explicitly including the copula parameter in the variance-covariance structure, our adjusted confidence intervals provide robust coverage probability under small samples and strong dependence—conditions where traditional methods can deviate from the nominal level.

Numerical experiments revealed that, while the traditional confidence intervals often remain close to their nominal coverage probability under moderate dependence or larger samples, they may underestimate variability in more challenging scenarios. In contrast, we found the proposed confidence intervals consistently maintain near-nominal coverage probability, even with up to 25% censoring. These findings underscore the practical gains from fully modeling both observed and unobserved heterogeneity, especially in high-dependence or data-sparse applications.

We further illustrated our analysis in a penalized estimation study with a synthetic real-like example, where we simulated data under nominal parameters $(\lambda_1, \lambda_2, \eta, \theta)$ but observed an unexpected pattern of early failures. This real-like scenario demonstrated how the maximum likelihood method can fail to produce invertible Hessian matrices, whereas a ridge-penalized approach successfully delivered finite standard errors—even though the resulting parameter estimates were substantially biased. Such findings confirm the importance of penalization or other stabilizing strategies whenever strong dependence and small samples are identified.

Although our study focused on two-component systems connected in series, extending this study to higher-dimensional settings is feasible but will face additional identifiability and computational complexities. Likewise, while we employed the Weibull distribution for its flexibility and frequent use in reliability contexts, alternative baselines (such as the exponential, gamma, or Birnbaum-Saunders distributions [43]) could be explored if data or expert knowledge suggests different hazard shapes. Moreover, although we illustrated the Gumbel and Clayton copulas for positive dependence, our framework accommodates other families, especially those capturing distinct tail behaviors, to match real-world failure patterns more closely.

Despite the strengths identified in our study, certain limitations remain. Greater systems may require stronger identifiability constraints or Bayesian/regularization strategies to separate frailty from copula effects reliably.

Further research could also examine semiparametric baselines and alternative censoring schemes [44,45]. Nonetheless, we believe that the proposed adjusted confidence intervals, by integrating both frailty and direct copula dependence, constitute a valuable tool for practical reliability analyses where correlated failures and small samples pose challenges, and that penalized variants of our estimation strategy offer a pragmatic fallback in highly demanding scenarios.

Author Contributions: All authors contributed to the conceptualization, methodology, and investigation of this research. Osnamir E. Bru-Cordero focused on the theoretical framework for frailty models and copula-based dependence structures, under the scientific supervision of Mario C. Jaramillo-Elorza and Víctor Leiva. Cecilia Castro led the overarching review and editing process, performed additional analyses, restructured the manuscript, and coordinated revisions in response to feedback. Víctor Leiva led the writing of the initial draft and subsequent revisions until the final submission. Mario C. Jaramillo-Elorza and Víctor Leiva supervised the overall study design, including the simulation scenarios and the critical review of the manuscript. All authors reviewed the results and approved the final version of the manuscript.

Availability of Data and Materials: The codes and data are available under request from the authors.

Ethics Approval: Not applicable. The research does not involve human or animal subjects.

Conflicts of Interest: The authors declare no conflicts of interest to report regarding the present study.

Appendix A R Script for Penalized Estimation and CI$_{\text{Dep}}$

This appendix provides an illustrative R script implementing data generation via a gamma-frailty Gumbel-copula model, quasi-Newton parameter estimation with a mild ridge penalty when the Hessian is nearly singular, and the construction of CI$_{\text{Dep}}$. For brevity, the code omits the routines for CI$_{\text{ML}}$ and CI$_{\text{Logit}}$, which can be coded analogously.

```r
#########################################################################
## R code  implementing:
##  - Gamma-frailty + Gumbel copula data generation
##  - Quasi-Newton parameter estimation with mild ridge penalty if Hessian
##    is nearly singulard
##  - Confidence intervals for the marginal quantile of mode 1 (CI_Dep)
##  - (Placeholders for CI_ML and CI_Logit are omitted
# for brevity in this script.)
#########################################################################

library(copula)
library(numDeriv)

#-----------------------------------------------------------------------
# 1) Data generation:
# two-component series system with gamma frailty + Gumbel copula
#-----------------------------------------------------------------------
simulate_series_data <- function(
    n,
    alpha1  = 1.2, alpha2  = 1.2,
    lambda1 = 40,   lambda2 = 20,
    eta     = 0.3,
    theta   = 2,
    cens_rate= 0
) {
  # Gamma frailty Z_i
  Z <- rgamma(n, shape = 1/eta, scale = eta)

  # Gumbel copula for (U1, U2)
  gC <- gumbelCopula(param = theta, dim = 2)
  U  <- rCopula(n, gC)
  u1 <- U[, 1]
  u2 <- U[, 2]
  # Weibull times, conditioned on Z
  T1 <- (lambda1 / Z^(1/alpha1)) * (-log(u1))^(1/alpha1)
  T2 <- (lambda2 / Z^(1/alpha2)) * (-log(u2))^(1/alpha2)
  # Observed time, cause
  Tobs  <- pmin(T1, T2)
  cause <- ifelse(T1 < T2, 1, 2)
  # Optional right-censoring from Exp(cens_rate)
  if(cens_rate > 0) {
    C <- rexp(n, rate = cens_rate)
    Tobs  <- pmin(Tobs, C)
    delta <- as.numeric(Tobs < C)
    # cause=0 if censored
    cause <- ifelse(delta == 1, cause, 0)
  }
  data.frame(time = Tobs, cause = cause)
}
#-----------------------------------------------------------------
# 2) Gumbel copula and gamma frailty density
#-----------------------------------------------------------------
CopulaGumbel <- function(u, v, theta) {
```

```
54    out      <- numeric(length(u))
55    idxOut <- (u <= 0 | u >= 1 | v <= 0 | v >= 1)
56    out[idxOut] <- 0
57    idxIn <- !idxOut
58    if(any(idxIn)) {
59       uu    <- u[idxIn]
60       vv    <- v[idxIn]
61       part <- ((-log(uu))^theta + (-log(vv))^theta)^(1/theta)
62       val  <- exp(-part)
63       val[!is.finite(val)] <- 0
64       out[idxIn] <- val}
65    out}
66  dFragGamma <- function(z, eta) {
67    k     <- 1/eta
68    coef <- 1/(gamma(k)*eta^k)
69    out  <- coef * z^(k-1)*exp(-z/eta)
70    out[z<=0]            <- 0
71    out[!is.finite(out)] <- 0
72    out}
73  #-----------------------------------------------------------------------
74  # 3) Joint survival S_joint(t1,t2) by integrating over gamma frailty
75  #-----------------------------------------------------------------------
76  S_joint <- function(t1, t2,
77                      alpha1, lambda1,
78                      alpha2, lambda2,
79                      eta, theta)
80  {
81    # If either time <=0, define survival=1 (convention)
82    if(t1 <= 0 || t2 <= 0) return(1)
83    integrand <- function(zval) {
84      sapply(zval, function(z0){
85        if(z0 <= 0) return(0)
86        # Protect exponent
87        u <- exp(-pmin(700, z0*(t1/lambda1)^alpha1))
88        v <- exp(-pmin(700, z0*(t2/lambda2)^alpha2))
89        cval <- CopulaGumbel(u, v, theta)
90        dval <- dFragGamma(z0, eta)
91        valz <- cval * dval
92        if(!is.finite(valz)) valz <- 0
93        valz
94      })}
95    val <- integrate(integrand, lower=0, upper=Inf, rel.tol=1e-6)$value
96    if(!is.finite(val)) val <- 0
97    max(val, 1e-15)
98  }
99  #-----------------------------------------------------------------------
100 # 4) f1(t) and f2(t) = partial derivatives of S_joint(t,t) w.r.t. t
101 #-----------------------------------------------------------------------
102 f1_t <- function(t, alpha1, lambda1,
```

```
103                     alpha2, lambda2,
104                     eta, theta)
105 { fx <- function(x){
106     S_joint(x, x, alpha1, lambda1, alpha2, lambda2, eta, theta) }
107   dval <- grad(fx, x=t, method="simple", method.args=list(eps=1e-6))
108   val  <- -dval
109   if(!is.finite(val)) val <- 1e-15
110   max(val, 1e-15)}
111 f2_t <- function(t, alpha1, lambda1,
112                     alpha2, lambda2,
113                     eta, theta)
114 { fy <- function(y){
115     # Here we swap alpha1/lambda1 with alpha2/lambda2
116     S_joint(y, y, alpha2, lambda2, alpha1, lambda1, eta, theta)
117   }
118   dval <- grad(fy, x=t, method="simple", method.args=list(eps=1e-6))
119   val  <- -dval
120   if(!is.finite(val)) val <- 1e-15
121   max(val, 1e-15)}
122 #------------------------------------------------------------------
123 # 5) Negative LL (no penalty)
124 #------------------------------------------------------------------
125 negloglik_dep <- function(par, data,
126                           alpha1 = 1.2,
127                           alpha2 = 1.2)
128 { lambda1 <- exp(par[1])
129   lambda2 <- exp(par[2])
130   eta     <- exp(par[3])
131   theta   <- 1 + exp(par[4])
132   nll <- 0
133   for(i in seq_len(nrow(data))) {
134     ti <- data$time[i]
135     cs <- data$cause[i]
136     if(cs == 1) {
137       ff <- f1_t(ti, alpha1, lambda1, alpha2, lambda2, eta, theta)
138       nll <- nll - log(max(ff, 1e-15))
139     } else if(cs == 2) {
140       ff <- f2_t(ti, alpha1, lambda1, alpha2, lambda2, eta, theta)
141       nll <- nll - log(max(ff, 1e-15))
142     } else {
143       ss <- S_joint(ti, ti, alpha1, lambda1, alpha2, lambda2, eta, theta)
144       nll <- nll - log(max(ss, 1e-15))
145     } }
146   nll
147 }
148 #------------------------------------------------------------------
149 # 6) Mild ridge penalty if Hessian is near-singular
150 #------------------------------------------------------------------
151 negloglik_dep_pen <- function(par, data,
```

```
152                                         alpha1=1.2, alpha2=1.2,
153                                         lambda_pen=1e-4)
154  {
155    base_val <- negloglik_dep(par, data, alpha1, alpha2)
156    # Ridge penalty => + (lambda_pen/2)*||par||^2
157    base_val + (lambda_pen * sum(par^2))/2
158  }
159  #----------------------------------------------------------------------
160  # 7) Quasi-Newton estimation: tries normal then re-tries w/ penalty
161  # if needed
162  #----------------------------------------------------------------------
163  fit_model_dep <- function(
164      data,
165      alpha1   = 1.2,
166      alpha2   = 1.2,
167      start_par= c(log(40), log(20), log(0.3), log(0.3)),
168      lambda_pen= 1e-4)
169  {
170    # First pass, no penalty
171    res_opt <- optim(
172      par      = start_par,
173      fn       = negloglik_dep,
174      data     = data,
175      alpha1   = alpha1,
176      alpha2   = alpha2,
177      method   = "BFGS",
178      hessian  = TRUE,
179      control  = list(maxit=500, reltol=1e-8))
180    # Check Hessian definiteness or near-singularity
181    H <- res_opt$hessian
182    ok_hessian <- TRUE
183    if(any(is.na(H)) || abs(det(H)) < 1e-10) {
184      ok_hessian <- FALSE}
185    # If near-singular, re-run with mild penalty
186    if(!ok_hessian) {
187      res_opt_pen <- optim(
188        par      = res_opt$par,
189        fn       = negloglik_dep_pen,
190        data     = data,
191        alpha1   = alpha1,
192        alpha2   = alpha2,
193        method   = "BFGS",
194        hessian  = TRUE,
195        control  = list(maxit=500, reltol=1e-8),
196        lambda_pen = lambda_pen)
197      # Compare final objective values
198      if(res_opt_pen$value < res_opt$value) {
199        return(list(
200          par           = res_opt_pen$par,
```

```
201        hessian      = res_opt_pen$hessian,
202        convergence = res_opt_pen$convergence,
203        value        = res_opt_pen$value,
204        penaltyUsed = TRUE
205      )) }}
206   # Otherwise return the original fit
207   list(
208     par          = res_opt$par,
209     hessian      = res_opt$hessian,
210     convergence = res_opt$convergence,
211     value        = res_opt$value,
212     penaltyUsed = FALSE
213   )}
214 #---------------------------------------------
215 # 8) Marginal quantile for mode 1
216 #---------------------------------------------
217 marginal_quantile_mode1 <- function(par, alpha1=1.2, p=0.5)
218 { lambda1 <- exp(par[1])
219   eta      <- exp(par[3])
220   A        <- ((1 - p)^(-eta) - 1) / eta
221   lambda1 * (A)^(1/alpha1)}
222 #-------------------------------------------------------------
223 # 9) Delta-method CI for the marginal quantile of mode 1 => CI_Dep
224 #-------------------------------------------------------------
225 quantileCI_mode1 <- function(
226     fit,
227     alpha1 = 1.2,
228     p      = 0.5,
229     level  = 0.95)
230 {   H <- fit$hessian
231   if(any(is.na(H))) return(c(NA, NA))
232   invH <- try(solve(H), silent=TRUE)
233   if(inherits(invH,"try-error")) return(c(NA, NA))
234   gfun <- function(pa){
235     tt <- marginal_quantile_mode1(pa, alpha1=alpha1, p=p)
236     log(tt)}
237   parhat  <- fit$par
238   ghat    <- gfun(parhat)
239   grad_g  <- grad(gfun, parhat, method="simple", method.args=list(eps=1e-6))
240   var_g   <- as.numeric(t(grad_g) %*% invH %*% grad_g)
241   if(is.na(var_g) || var_g < 0) return(c(NA, NA))
242   se_g  <- sqrt(var_g)
243   zc    <- qnorm(1 - (1 - level)/2)
244   ci_ln <- c(ghat - zc*se_g, ghat + zc*se_g)
245   exp(ci_ln)}
246 #-----------------------------------------------------------------
247 # 10) Coverage simulation for the Dep-based interval (CI_Dep).
248 #     (CI_ML, CI_Logit would be coded similarly but are omitted here.)
249 #-----------------------------------------------------------------
```

```r
250  simulate_coverage_dep <- function(
251      n, B=50,
252      alpha1=1.2, alpha2=1.2,
253      lambda1=40, lambda2=20,
254      eta=0.3, theta=2,
255      p=0.5,
256      cens_rate=0,
257      lambda_pen=1e-4
258  )
259
260  {
261    # "True" marginal quantile for mode 1
262    true_tp_fun <- function(p, alpha, lambda, eta){
263      A <- ((1 - p)^(-eta) - 1) / eta
264      lambda*(A)^(1/alpha)
265    }
266    tp_real <- true_tp_fun(p, alpha1, lambda1, eta)
267
268    covers <- numeric(B)
269    for(b in seq_len(B)) {
270      dat_b <- simulate_series_data(
271        n         = n,
272        alpha1    = alpha1, alpha2 = alpha2,
273        lambda1   = lambda1, lambda2= lambda2,
274        eta       = eta,     theta  = theta,
275        cens_rate= cens_rate
276      )
277
278      # Fit the model with possible ridge if Hessian is near-singular
279      fit_b <- fit_model_dep(dat_b, alpha1=alpha1, alpha2=alpha2,
280                             lambda_pen=lambda_pen)
281      ci_b  <- quantileCI_mode1(fit_b, alpha1=alpha1, p=p)
282
283      if(any(is.na(ci_b))) {
284        covers[b] <- NA
285      } else {
286        covers[b] <- as.numeric(tp_real >= ci_b[1] && tp_real <= ci_b[2])
287      }
288    }
289    mean(covers, na.rm=TRUE)
290  }
```

References

1. Li H, Peng W, Adumene S, Yazdi M. Cutting edge research topics on system safety, reliability, maintainability, and resilience of energy-critical infrastructures. In: Intelligent reliability and maintainability of energy infrastructure assets. Cham, Switzerland: Springer; 2023. p. 25–38 doi:10.1007/978-3-031-29962-9_2.

2. Osei-Kyei R, Almeida LM, Ampratwum G, Tam V. Systematic review of critical infrastructure resilience indicators. Constr Innov. 2023;23(5):1210–31. doi:10.1108/ci-03-2021-0047.

3. Li Y, Bai X, Shi S, Wang S. Dynamic fatigue reliability analysis of transmission gear considering failure dependence. Comput Model Eng Sci. 2022;130(2):1077–92. doi:10.32604/cmes.2022.018181.

4. Livingston D, Sivaram V, Freeman M, Fiege M. Applying blockchain technology to electric power systems. New York, NY, USA: Council on Foreign Relations; 2022.

5. Giraldo R, Leiva V, Christakos G. Leverage and Cook distance in regression with geostatistical data: methodology, simulation, and applications related to geographical information. Int J Geogr Inf Sci. 2023;37(3):607–33. doi:10.1080/13658816.2022.2131790.

6. Aven T, Jensen U. Stochastic failure models. In: Stochastic models in reliability. New York, NY, USA: Springer; 2013. p. 57–103.

7.   Wagner N. Comparing the complexity and efficiency of composable modeling techniques for multi-scale and multi-domain complex system modeling and simulation applications: a probabilistic analysis. Systems. 2024;12(3):96. doi:10.3390/systems12030096.

8.   Qiu J, Sun H, Wang S. Research progress of reverse Monte Carlo and its application in Josephson junction barrier layer. Comput Model Eng Sci. 2023;137(3):2077–109. doi:10.32604/cmes.2023.027353.

9.   Wang C. Structural reliability and time-dependent reliability. Cham, Switzerland: Springer; 2021.

10. Guiraud P, Leiva V, Fierro R. A non-central version of the Birnbaum-Saunders distribution for reliability analysis. IEEE Trans Reliab. 2009;58(1):152–60. doi:10.1109/tr.2008.2011869.

11. Netes V, Sharov V. Common cause failures in communication networks. In: Proceedings of the 2024 Conference on Systems of Signals Generating and Processing in the Field of on Board Communications; 2024 Mar 12–14; Moscow, Russian Federation. p. 1–7.

12. Meeker WQ, Escobar LA, Pascual FG. Statistical methods for reliability data. New York, NY, USA: Wiley; 2022.

13. Octavina S, Lin SW, Yeh RH. Copula-based Bayesian reliability assessment for series systems. Qual Reliab Eng Int. 2024;40(5):2444–55. doi:10.1002/qre.3514.

14. Abuelamayem O. Reliability estimation of a multicomponent stress-strength model based on copula function under progressive first failure censoring. Stat Optim Inf Comput. 2024;12(6):1601–11. doi:10.19139/soic-2310-5070-1894.

15. Zheng M, Klein JP. Estimates of marginal survival for dependent competing risks based on an assumed copula. Biometrika. 1995;82(1):127–38. doi:10.1093/biomet/82.1.127.

16. Barlow R, Proschan F. Statistical theory of reliability and life testing: probability models. New York, NY, USA: Wiley; 1975.

17. Navarro J, Durante F. Copula-based representations for the reliability of the residual lifetimes of coherent systems with dependent components. J Multivar Anal. 2017;158:87–102. doi:10.1016/j.jmva.2017.04.003.

18. Nelsen RB. An introduction to copulas. New York, NY, USA: Springer; 2006.

19. Leiva V, dos Santos RA, Saulo H, Marchant C, Lio Y. Bootstrap control charts for quantiles based on log-symmetric distributions with applications to the monitoring of reliability data. Qual Reliab Eng Int. 2023;39(1):1–24. doi:10.1002/qre.3072.

20. Aalen O, Borgan O, Gjessing H. Survival and event history analysis: a process point of view. New York, NY, USA: Springer; 2008.

21. Mokkink LB, de Vet H, Diemeer S, Eekhout I. Sample size recommendations for studies on reliability and measurement error: an online application based on simulation studies. Health Serv Outcomes Res Methodol. 2023;23(3):241–65. doi:10.1007/s10742-022-00293-9.

22. Brown B, Liu B, McIntyre S, Revie M. Reliability evaluation of repairable systems considering component heterogeneity using frailty model. Proc Inst Mech Eng O J Risk Reliab. 2023;237(4):654–70. doi:10.1177/1748006x221109341.

23. Gorfine M, Zucker DM. Shared frailty methods for complex survival data: a review of recent advances. Annu Rev Stat Appl. 2023;10(1):51–73. doi:10.1146/annurev-statistics-032921-021310.

24. Wang YC, Emura T, Fan TH, Lo SM, Wilke RA. Likelihood-based inference for a frailty-copula model based on competing risks failure time data. Qual Reliab Eng Int. 2020;36(5):1622–38. doi:10.1002/qre.2650.

25. Leao J, Leiva V, Saulo H, Tomazella V. Incorporation of frailties into a cure rate regression model and its diagnostics and application to melanoma data. Stat Med. 2018;37(29):4421–40. doi:10.1002/sim.7929.

26. Calsavara VF, Tomazella V, Fogo JC. The effect of frailty term in the standard mixture model. Chil J Stat. 2013;4(2):95–109.

27. Wang YC, Emura T. Multivariate failure time distributions derived from shared frailty and copulas. Jpn J Stat Data Sci. 2021;4(2):1105–31. doi:10.1007/s42081-021-00123-1.

28. Rouzbahani M, Akhoond MR, Chinipardaz R. A new bivariate survival model with a cured fraction: a mixed Poisson frailty-copula approach. Jpn J Stat Data Sci. 2025;11(4):261. doi:10.1007/s42081-023-00240-z.

29. Liu X. Planning of accelerated life tests with dependent failure modes based on a gamma frailty model. Technometrics. 2012;54(4):398–409. doi:10.1080/00401706.2012.707579.

30. Lu JC, Bhattacharyya GK. Some new constructions of bivariate Weibull models. Ann Inst Stat Math. 1990;42(3):543–59. doi:10.1007/bf00049307.

31. Murthy DP, Xie M, Jiang R. Weibull models. New York, NY, USA: Wiley; 2004.

32. Escarela G, Carriere J. Fitting competing risks with an assumed copula. Stat Methods Med Res. 2003;12(4):333–49. doi:10.1191/0962280203sm335ra.

33. Duchateau L, Janssen P. The frailty model. New York, NY, USA: Springer; 2007.

34. Ibrahim JG, Chen MH, Sinha D. Bayesian survival analysis. Hoboken, NJ, USA: Wiley; 2014.

35. Tableman M, Kim JS. Survival analysis using S: analysis of time-to-event data. Boca Raton (FL): CRC Press; 2003.

36. Hougaard P. Analysis of multivariate survival data. New York, NY, USA: Springer; 2012.

37. Lin H, Zelterman D. Modeling survival data: extending the cox model. New York, NY, USA: Taylor and Francis; 2002.

38. Wienke A. Frailty models in survival analysis. Boca Raton, FL, USA: Chapman & Hall/CRC; 2010.

39. Hong Y, Meeker WQ. Confidence intervals for system reliability and applications to competing risks models. Lifetime Data Anal. 2014;20(2):161–84. doi:10.1007/s10985-013-9245-9.

40. Vallejos CA, Steel MF. Incorporating unobserved heterogeneity in Weibull survival models: a Bayesian approach. Econom Stat. 2017;3(2):73–88. doi:10.1016/j.ecosta.2017.01.005.

41. Emura T, Nakatochi M, Murotani K, Rondeau V. A joint frailty-copula model between tumour progression and death for meta-analysis. Stat Methods Med Res. 2017;26(6):2649–66. doi:10.1177/0962280215604510.

42. Tsiatis A. A nonidentifiability aspect of the problem of competing risks. Proc Natl Acad Sci USA. 1975;72(1):20–2. doi:10.1073/pnas.72.1.20.

43. Leiva V, Castro C, Vila R, Saulo H. Unveiling patterns and trends in research on cumulative damage models for statistical and reliability analyses: bibliometric and thematic explorations with data analytics. Chil J Stat. 2024;15:81–109.

44. Barros M, Leiva V, Ospina R, Tsuyuguchi A. Goodness-of-fit tests for the Birnbaum-Saunders distribution with censored reliability data. IEEE Trans Reliab. 2014;63(2):543–54. doi:10.1109/tr.2014.2313707.

45. Cárcamo E, Marchant C, Ibacache-Pulgar G, Leiva V. Birnbaum-Saunders semi-parametric additive modeling: estimation, smoothing, diagnostics and application. REVSTAT Stat J. 2024;22:211–37. doi:10.57805/revstat.v22i2.483.